Supporting information for the manuscript:

Multiple Click-Selective tRNA Synthetases Expand Mammalian Cell-Specific Proteomics

Andrew C. Yang,[†,§,‡] Haley du Bois,[‡] Niclas Olsson,[⊥] David Gate,[‡] Benoit Lehallier,[‡] Daniela Berdnik,[‡,¶] Kyle D. Brewer,[§,‡] Carolyn R. Bertozzi,[§,∣,//] Joshua E. Elias,[⊥] Tony Wyss-Coray[*,‡,¶]

† Department of Bioengineering, § Chemistry, Engineering, and Medicine for Human Health (ChEM-H), ‡ Department of Neurology and Neurological Sciences, ⊥ Department of Chemical and Systems Biology, ∣ Department of Chemistry, // Howard Hughes Medical Institute, Stanford University, Stanford, California 94305, USA

¶ Center for Tissue Regeneration, Repair and Restoration, V.A. Palo Alto Healthcare System, Palo Alto, California, 94304, USA

Materials and Methods:

Cloning of synthetase variants into mammalian vectors. Mouse or human codon-optimized variants of *Sc*Tyr$_{Y43G}$, *Mm*Phe$_{T413G}$, and wild-type PheRS were ordered as gBlocks (IDT), with NheI and EcoRI restriction sites in the N- and C-terminus, respectively (sequences in Figure S1). gBlock sequences were PCR amplified, cleaned, and digested with NheI and EcoRI before insertion into the multiple cloning site of the Piggybac vector PB513B-1 (SBI). The *CP1 switch* construct was created by replacing the *E. coli* TyRS CP1 domain (amino acids 385-583) with that of the human TyRS, and cloned into PB513B-1[1]. In this vector, the inserted transgene is driven by the CMV promoter, with GFP and puromycin gene expressed via an EF1α promoter. The *MjTyRS* construct was obtained via PCR of the synthetase from the pEVOL-pAzF plasmid (Addgene), and cloned into PB513B-1. We used Stable Competent *E. coli* (NEB) for transformations, 100 μg/ml ampicillin for colony selection, and the HiSpeed Plasmid Maxi Kit (Qiagen) for DNA purification.

Cell culture. HEK293T and B16-F10 cells were cultured in DMEM (Invitrogen) medium with 10% fetal bovine serum (FBS). CHO-K1 cells were cultured in Ham's F-12K Medium (Kaighn's, Thermo) medium with 10% fetal bovine serum. All cells were passaged every two to three days on tissue-culture plates, incubating at 37°C and 5% CO2, and discarded before reaching passage 18.

Cell transfection, click amino acid labeling, and selection of stably transfected B16-F10 cells. Unless otherwise noted, cells were transiently transfected with Lipofectamine 3000 (Invitrogen) 24 hours prior to 4-Azido-L-phenylalanine (AzF, Chem-Implex) or 3-Azido-L-tyrosine (AzY, Watanabe Chemical Industries) labeling. For initial assessment of labeling across mammalian cell lines, transfected cells were incubated with 2 mM of AzF, AzY, tyrosine, or phenylalanine for 30 hours in 12-well plates prior to lysis. To characterize enzyme selectivity and rate of substrate activation, transfected HEK293T cells were incubated with varying amounts of endogenous and non-canonical amino acids for 24 hours in 12-well plates prior to lysis. For affinity enrichment prior to shotgun mass spectrometry, transfected HEK293T cells were incubated with 125 μM of endogenous and non-canonical amino acids for 24 hours in 10 cm dishes prior to lysis. B16-F10 cells were transfected with mutant synthetases in the Piggybac vector PB513B-1 for 72 hours prior to puromycin selection at 10 μg/ml for 10 days.

Copper-free reaction of DIBO-Alexa Fluor 647 with click-labeled cell lysates for in-gel fluorescence. After washing in PBS twice, cells were lysed 1% SDS in PBS with EDTA-free protease inhibitor (Roche). Lysates were sonicated with a tip sonicator to reduce sample viscosity before centrifugation at 14,000g for 20 minutes at 4°C. The supernatant was collected and kept at −80°C for long-term storage. Protein concentrations were measured with a BCA Protein Assay Kit (Pierce) to ensure equal loading across gel wells (~23 μg). Lysates were alkylated with 6 mM iodoacetamide (Pierce) for 45 minutes in the dark at room temperature, before the copper-free click reaction with DIBO-Alexa Fluor 647 (Thermo) for 90 minutes in the dark at room temperature. A 4x stock solution of NuPAGE LDS (Thermo) and 8% (v/v) 2-mercaptoethanol (Sigma) was added to each sample before heating at 95°C. Proteins were briefly spun and separated by electrophoresis in 12% Bis-Tris polyacrylamide gels (Invitrogen). Gels were washed twice in distilled water for 10 minutes before Alexa Fluor 647 imaging in the 700-nm channel of an Odyssey CLx (LI-COR). To assess protein loading, gels were incubated with GelCode Blue Stain Reagent (Thermo) overnight before destaining in distilled water for at least 3 hours. Colloidally stained gels were imaged in the 800-nm channel of an Odyssey CLx (LI-COR), where no bleed-through of the Alexa Fluor 647 signal was detected. Quantification of signal intensities of labeled proteomes from each gel lane were analyzed in ImageJ as before, but with slight modifications[2]. Specifically, individual lanes were not split into quarters to report intensity mean and standard deviations. Instead, the mean and standard deviations were calculated from biological triplicates of whole gel lanes, less the dye front.

Copper-catalyzed reaction of alkyne-Alexa Fluor 647 for microscopy. 10 hours after transfection, adherent HEK293T cells were plated onto glass bottom tissue culture plates (MatTek) and chambered coverglass (Nunc™ Lab-Tek™ Thermo) coated with CELLstart (Thermo). After

another 20 hours, adherent cells were incubated with 125 μM of endogenous or non-canonical amino acids for 12 hours. Cells were washed twice with PBS, fixed with 4% paraformaldehyde (VWR) for 15 minutes at room temperature, washed with PBS twice more, permeabilized with 0.1% Triton X-100 for 2 minutes at room temperature, and washed three times for 5 minutes each with PBS. Labeling was performed at room temperature for 2.5 hours in PBS with a final concentration of 0.1 mM copper sulfate, 0.5 mM THPTA (Click Chemistry Tools), 5 mM sodium ascorbate, 5 mM aminoguanidine and 10 μM alkyne-Alexa Fluor 647 (Thermo). Cells were washed five times for 5 minutes each before leaving in PBS overnight shaking at 4°C. Cells were then incubated with Hoechst 33342 Solution (Thermo) for 15 minutes to stain nuclei, washed three times with PBS for 5 minutes each, and mounted with ProLong Gold Antifade Mountant (Thermo). Fluorescence confocal images were obtained on a Zeiss LSM 880 microscope and KEYENCE BZ-X700 for quantification.

For imaging of B16-F10 *in vivo* melanoma slices, tumors were fixed for 48 hours in 4% paraformaldehyde before being embedded in 5% low-melt agarose (Sigma) and vibratome sectioned in PBS. Slices were blocked and permeabilized for 30 minutes in 6% BSA and 0.2% Triton X-100 before three washes in 1% BSA in PBS. Copper-click labeling, Hoechst staining, and mounting was performed as above before imaging on a Zeiss LSM 700 microscope.

Copper-free reaction of DIBO-Alexa Fluor 647 for flow cytometry. 30 hours after transfection, adherent HEK293T cells were incubated with 125 μM of endogenous or non-canonical amino acids for 16 hours. Cells were then suspended, washed twice with PBS, and incubated with LIVE/DEAD™ Fixable Violet Dead Cell Stain (Thermo), per manufacturer's instructions. Cells were washed once with PBS, fixed with 4% paraformaldehyde for 15 minutes at room temperature, washed three times with 1% FBS in PBS, and alkylated with 10 mM iodoacetamide in 1% FBS for 30 minutes in the dark at room temperature. Cells were then reacted with 6 μM DIBO-Alexa Fluor 647 for 2 hours. Cells were washed three times with 1% FBS in PBS and left in 1% FBS solution overnight shaking at 4°C. After a final wash in 1% FBS, cells were filtered through a 35 μM nylon mesh (Corning). Flow cytometry was performed using an LSRFortessa (BD), with only live/ dead-discriminated, single cells kept for analysis in FlowJo 10. DIBO 647+ cells were live/ dead-discriminated, singlets with Alexa Fluor 647 signal (a.u.) greater than $3*10^3$.

Affinity enrichment of AzF- or AzY-labeled proteins for mass spectrometry. Transfected HEK293T cells were incubated with 125 M of endogenous and non-canonical amino acids for 24 hours in triplicate 10 cm dishes prior to PBS washes and lysis. Endogenous amino acid samples were used to estimate the degree of non-specific enrichment. Cells were lysed in a solution of 1% SDS, 8 M urea, 1 M NaCl, 100 mM chloroacetamide, 20 mM iodoacetamide, and EDTA-free protease inhibitor (Roche). Lysates were sonicated with a tip sonicator to reduce sample viscosity before centrifugation at 14,000g for 20 minutes at 4°C. After ensuring uniform protein concentrations (3 mg of lysates) via BCA assay (Pierce), samples were pre-cleared with pre-washed 6% BCL agarose beads (ABT) for 90 minutes, rotating in the dark. Agarose beads were pre-washed three times with 0.8% SDS in PBS. Lysates were removed from plain agarose beads and each added to 50 μL of similarly pre-washed azadibenzocyclooctyne (DBCO) resin (50% slurry by volume; Click Chemistry Tools). The copper-free cycloaddition proceeded rotating, overnight, in the dark, at room temperature. As before, unreacted DBCO groups were quenched by the addition of 100 mM AnI for 30 minutes (2 mM final concentration)[3]. Supernatant was removed, beads washed with at least 1 mL of H_2O, reduced with 1 mL DTT (1 mM, 15 minutes at 70°C with occasional vortexing), and alkylated with 1 mL iodoacetamide (40 mM, 30 minutes at room temperature, in the dark). Beads were then washed with greater than 50 mL each of 0.8% SDS in PBS, 8 M urea in 100 mM Tris (pH 8), and 20% acetonitrile. The resin was resuspended in 1 mL of 50 mM HEPES and transferred to an eppendorf tube. After centrifugation at 1,000g for 5 minutes and removal of ~750 uL of supernatant, 1 μg of Mass Spec Grade Trypsin/Lys-C Mix was added to each sample (Promega). Samples were digested overnight at 37°C, the beads spun, and supernatant collected.

Mass spectrometry. Peptides eluted from DBCO enrichment of HEK293T cell lysates were labelled with 10-plex Tandem Mass Tags (TMT) (Thermo Scientific) per manufacturer's instructions. A global

standard was created by taking an equal aliquot of each peptide sample and included in each 10-plex. A subset of each sample and the standard was removed to check reporter ion distributions and TMT labeling efficiency. The remainder were mixed with the adjusted ratio, dried down, resuspended in 0.1% formic acid, cleaned using C18-based STAGE Tips, lyophilized, and stored at −80 °C until final LC–MS/MS measurement[4,5]. Peptides were analyzed on an LTQ Orbitrap Fusion Tribrid Mass Spectrometer (Thermo Scientific). Peptides were separated by capillary reverse-phase chromatography on a 24 cm reversed-phase column (100 µm inner diameter, packed in-house with ReproSil-Pur C18-AQ 3.0 m resin (Dr. Maisch)) over a total run time of 180 min using a four-step linear gradient via an Dionex Ultimate 3000 LC-system (Thermo Scientific): 97% A (and 3% B) to 96% A in 15 min, to 75% A in 135 min, to 55% A in 15 min, and then to 5% A in 15 min, where buffer A is 0.1 % formic acid in water; buffer B is 0.1 % formic acid in acetonitrile. Acquisition was performed in data-dependent mode with the full MS scans acquired in the Orbitrap mass analyzer with a resolution of 120,000 and m/z scan range 400–1,500. The AGC targets were $4*10^5$ and the maximum injection time for $FTMS^1$ were 50 ms. The most intense ions were then selected in top speed mode for sequencing using collision-induced dissociation (CID) and the fragments were analyzed in the ion trap. The normalized collision energy for CID was 35% at 0.25 activation Q. The AGC targets were $1*10^4$ and the maximum injection time for MS^2 were 30 ms. Monoisotopic precursor selection and charge state rejection were enabled. Singly charged ion species and ions with no unassigned charge states were excluded from MS2 analysis. Ions within ±10 ppm m/z window around ions selected for MS2 were excluded from further selection for fragmentation for 90 s. Following each MS2 analysis, five most intense fragment ions were selected simultaneously for HCD MS3 analysis with isolation width of 1.2 m/z, normalized collision energy of 65% at resolution of 60,000, AGC target were $1*10^5$ and maximum injection time of 90 ms. The raw data files were processed and analyzed using Proteome Discoverer software v2.1 (Thermo). Precursor mass tolerance is set to ±10 ppm and fragment mass tolerance is set to ±0.6 Da. Carbamidomethylation of cysteine (+57.021 Da), TMT-labeled N-terminus and lysine (+229.163) were set as static modifications. Differential modifications were: oxidation of methionine (+15.995 Da), phosphorylation of serine, tyrosine and threonine (+79.9663), acetylation of protein N-terminal (+42.011 Da). Proteome Discoverer searched the spectra against the Uniprot Human database (June 2016) including common contaminants using the SEQUEST algorithm.[6] Percolator was applied to filter out the false MS2 assignments at a strict false discovery rate of 1% at both the peptide and protein level.[7] For quantification, a mass tolerance of ±20 ppm window was applied to the integration of report ions using the most confident centroid method. Protein abundance was estimated by taking the average abundance of the top 3 peptides mapped to that protein.

For data preprocessing of TMT-labeled samples, the mean of two technical replicates was used for each biological replicate. Intensities were normalized to the global TMT standard. Statistical analysis was performed on 1539 proteins with signal in at least one sample. Because missing data must be imputed for principal component analysis (PCA), missing data for each protein were imputed conservatively by taking the lowest value across replicates where data was present and dividing by 2. Normed PCA was performed using the R ade4 package.[8] For differential expression analysis, non-imputed data was compared between groups using the Welch Two Sample t-test, when $n \geq 2$ in each group. The venn diagram represents the number of significantly detectable proteins ($p<0.05$) with $|\log_2(FC)|>1$. Volcano plots represent the pairwise comparison of hits between mutants; or in Figure S6, between ncAA-fed and canonical amino acid-fed conditions. The heatmap represents genes significantly detectable by at least one mutant ($p<0.05$).

For enriched *in vivo* melanoma and plasma samples, peptides were prepared as above, excluding TMT-specific adaptations, and analyzed on an LTQ Orbitrap Elite mass spectrometer (Thermo Fisher Scientific). Samples were separated by capillary reverse-phase chromatography on a 24-cm reversed-phase column (100 µm inner diameter, packed in-house with ReproSil-Pur C18-AQ 3.0 m resin (Dr. Maisch)) over a total run time of 160 min using a two-step linear gradient with 4–25% buffer B (0.2% (v/v) formic acid, 5% DMSO, and 94.8% (v/v) acetonitrile) for 120 min followed by 25–40% buffer B for 30 min using an Eksigent ekspert nanoLC-425 system (SCIEX, Framingham,

Massachusetts, USA). Acquisition was executed in data-dependent mode with the full MS scans acquired in the Orbitrap mass analyser with a resolution of 60,000 and m/z scan range 340–1,600. The top 20 most abundant ions with intensity threshold above 500 counts and charge states 2 and above were selected for fragmentation using collision- induced dissociation (CID) with isolation window of 2 m/z, collision energy of 35%, activation Q of 0.25 and activation time of 5 ms. The CID fragments were analyzed in the ion trap with rapid scan rate. Dynamic exclusion was enabled with repeat count of 1 and exclusion duration of 30 s. The AGC target was set to $1*10^6$ and 5000 for full FTMS scans and ITMSn scans. The maximum injection time was set to 250 s and 100 s for full FTMS scans and ITMSn scans. Data analysis was performed as above using Proteome Discoverer software v2.2 (Thermo), excluding TMT-specific adaptations. Peptide intensities were analyzed with Excel and Perseus.[9] Labeled proteins were identified adopting previous methods.[10] Briefly, only proteins detected (1) exclusively in the *Sc*Tyr$_{Y43G}$+AzY or *Mm*Phe$_{T413G}$+AzF replicates (and not in *Sc*Tyr$_{Y43G}$+Y or *Mm*Phe$_{T413G}$+F control replicates); or (2) found across all replicates and ≥5 times enriched in the *Sc*Tyr$_{Y43G}$+AzY or *Mm*Phe$_{T413G}$+AzF replicates were considered labeled. Labeled proteins were annotated using STRAP and Ingenuity Pathway Analysis (Qiagen) software.[11,12]

Codon usage analysis. To determine whether *Sc*Tyr$_{Y43G}$ and *Mm*Phe$_{T413G}$ can load both of their cognate codons (TAT and TAC for *Sc*Tyr$_{Y43G}$; and TTT and TTC for *Mm*Phe$_{T413G}$), cDNA sequences of TMT-quantified HEK293T proteins were retrieved via the Ensembl human genome database (Human release 92). cDNA sequences were parsed into codon triplets and the number of the four aforementioned codons counted for each protein. Proteins with exclusively one of the two tyrosine or phenylalanine codons (e.g., TAT only) were mapped against proteins significantly enriched by *Sc*Tyr$_{Y43G}$+AzY and *Mm*Phe$_{T413G}$+AzF. This yielded a list of proteins that were labeled by *Sc*Tyr$_{Y43G}$ or *Mm*Phe$_{T413G}$ uniquely via that codon. To assess whether labeling was preferential between cognate codons, codon fractions of significantly enriched proteins were compared with the codon fractions of all TMT-identified proteins.

Animals and B16-F10 melanoma tumor model. Female C57BL/6 mice were purchased from Charles River and kept on a 12-h light/dark cycle and provided access to food and water *ad libitum*. All animal procedures complied with the Animal Welfare Act and were in accordance with institutional guidelines by the V.A. Palo Alto Committee on Animal Research and the institutional administrative panel of laboratory animal care at Stanford University. Stably transfected B16-F10 cells were suspended, washed in PBS twice, and checked for viability with trypan blue. Only cells with viabilities greater than 90% were considered for subsequent subcutaneous injection. Cells were filtered through a 100 μM strainer (Fisher), spun, and resuspended in DMEM at 10^7 cells/ml. 100 μL of cells (10^6 cells) were subcutaneously injected into the right hind limb of 12-week-old female mice. Animals were monitored for palpable tumor starting at 10 days after injection. 16 days post-injections, mice were administered 1 mmol/ kg of amino acid intraperitoneally and intratumorally. Intratumoral injection volumes of 25 mM stock solution were 1/5th of the caliper-measured tumor volume $V = \frac{W^2 L}{2}$, where W is tumor width and L is tumor length. On days 18-19, mice were anesthetized with 2.5% (v/v) avertin. Blood was collected with EDTA as anticoagulant by terminal intracardial bleeding. EDTA-plasma was isolated by centrifugation at 1,000g for 15 min at 4 °C before aliquoting, flash freezing, and storage at −80 °C. Tumors were excised, and the majority minced and filtered through a 100 μM strainer. Tumor cells were washed 3x in PBS via centrifugation at 500g for 10 min at 4 °C before flash freezing and storage at −80 °C. For affinity enrichment and mass spectrometry, approximately 3mg of tumor lysates and plasma were prepared as indicated above. Remaining tumor tissue was immersion fixed in 4% PFA for imaging.

Figure S1. DNA and protein sequences for *Sc*Tyr$_{Y43G}$, *Mm*Phe$_{T413G}$, and *Hs*Phe$_{T413G}$.

***Sc*Tyr$_{Y43G}$**

ATGTCCTCAGCTGCCACCGTTGATCCAAATGAAGCTTTTGGGTTGATAACAAAAAACCTCCAAG
AAGTGTTGAACCCTCAGATCATCAAGGATGTCCTTGAAGTACAAAAAAGGCATTTGAAGCTCGG
GTGGGGAACTGCCCCTACCGGGCGCCCACATTGTGGGTATTTCGTCCCTATGACTAAGTTGGC
TGATTTCTTGAAGGCAGGCTGCGAGGTGACTGTGCTCCTGGCCGACTTGCACGCCTTTTTGGA
TAATATGAAGGCCCCTCTCGAGGTCGTCAATTATCGAGCCAAGTACTACGAACTCACCATTAAA
GCAATCTTGAGGAGTATAAACGTCCCTATAGAAAAACTTAAATTTGTTGTAGGTTCTTCATATCAA
CTGACACCCGATTATACCATGGACATTTTTAGACTGAGCAACATTGTGTCCCAAAACGATGCTAA
AAGAGCAGGAGCTGACGTTGTGAAACAAGTTGCAAACCCACTTCTTTCAGGCCTGATATATCCT
CTTATGCAAGCACTCGACGAACAATTCCTTGATGTCGATTGCCAGTTCGGAGGTGTAGACCAGC
GAAAAATCTTTGTTTTGGCCGAAGAGAACCTGCCCTCTCTGGGCTATAAAAAACGGGCTCACTT
GATGAATCCAATGGTCCCCGGATTGGCCCAAGGTGGCAAAATGTCTGCATCAGACCCCAACTC
TAAAATAGATCTGCTGGAGGAACCAAAGCAAGTTAAGAAGAAAATTAACTCCGCCTTTTGCAGT
CCTGGCAATGTCGAGGAAAACGGGCTTCTGTCATTCGTGCAGTATGTGATCGCCCCAATTCAAG
AACTCAAGTTCGGTACAAATCATTTTGAGTTTTTTATAGATCGACCAGAAAAATTTGGGGGACCT
ATTACATACAAGAGTTTTGAAGAGATGAAATTGGCCTTCAAAGAAGAGAAGCTGAGCCCACCTG
ATCTGAAGATCGGAGTGGCCGACGCCATCAATGAGTTGCTTGAACCAATACGACAGGAATTTGC
TGATAACAAAGAGTTTCAGGAAGCTAGTGAAAAGGGCTATCCCGTAGCAACCCCACAAAAATCT
AAAAAAGCAAAAAAACCTAAGAATAAGGGTACTAAATACCCTGGGGCTACCAAGACTAATGAAA
TTGCTACTAAGCTGGAGGAGACTAAATTGTAATGATGATAA

MSSAATVDPNEAFGLITKNLQEVLNPQIIKDVLEVQKRHLKLGWGTAPTGRPHCGYFVPMTKLADFL
KAGCEVTVLLADLHAFLDNMKAPLEVVNYRAKYYELTIKAILRSINVPIEKLKFVVGSSYQLTPDYTMD
IFRLSNIVSQNDAKRAGADVVKQVANPLLSGLIYPLMQALDEQFLDVDCQFGGVDQRKIFVLAEENL
PSLGYKKRAHLMNPMVPGLAQGGKMSASDPNSKIDLLEEPKQVKKKINSAFCSPGNVEENGLLSFV
QYVIAPIQELKFGTNHFEFFIDRPEKFGGPITYKSFEEMKLAFKEEKLSPPDLKIGVADAINELLEPIRQ
EFADNKEFQEASEKGYPVATPQKSKKAKKPKNKGTKYPGATKTNEIATKLEETKL****

***Mm*Phe$_{T413G}$**

ATGGCAGACAACCCTGTTCTCGAACTGCTCTTGCGGCGGTTGGAAGTAGCAGATGGAGGTTTG
GATTCAGCAGAACTTGCCACCCAACTTGGCGTTGAACATCAGGCCGTCGTTGGGGCAGTGAAG
AGTCTGCAAGCACTCGGGGAGGTGATAGAGGCTGAGCTTAGAAGTACAAAATGCTGGGAGTTG
ACCACCGAGGGTGAAGAGATTGCTAGAGAAGGGAGTCACGAGGCACGCGTTTTTCGGAGTATA
CCTCTTGAAGGACTTGTGCAGTCAGAATTGATGCACCTTCCCTCAGGTAAGGTTGGATTTAGTA
AAGCCATGAGTAATAAATGGATAAGAGTTGATAAATCAGCCGCCGACGGGCCAAGGGTGTTTA
GAGTCGTCGATTCTATAGAGGATGAAGTACAGAAAAGACTCCAACTGGTTCAGGCTGGACAAG
CAGAAAAGCTCGCAGAAAAAGAACGGAATGAATTGAGAAAACGCAAACTGCTGACCGAAGTGA
TTTTGAAAACATATTGGGTTTCAAAGGGGAAAGCATTTTCCACATCAGTGTCTAAGCAAGAAGCC
GAGCTCTCCCCTGAAATGATTTCTAGCGGAAGTTGGCGGGACCGACCATTCAAACCTTATAATT
TCAGCGCAAGGGGAGTCCTTCCAGATTCAGGCCACCTCCACCCTCTTCTTAAAGTCCGCTCCC
AGTTCCGGCAGATCTTTCTGGAGATGGGGTTCACAGAAATGCCTACTGACAATTTTATTGAGTC
TAGCTTTTGGAATTTCGACGCACTCTTCCAGCCCCAACAGCACCCCGCAAGAGACCAACACGA
CACATTTTTTCTCAGGGATCCTGCTGAAGCTCTCCAATTGCCAATGGGATACGTTCAGAGGGTG
AAGAGAACTCATTCACAAGGAGGATATGGTTCTCAGGGATATAAGTACACCTGGAAGTTGGAAG
AGGCTAGGAAAAATCTCTTGCGGACTCACACTACAGCCGCCTCCGCTCGCGCTCTGTATCAGC
TCGCACAAAAAAAGCCTTTCACCCCAGCAAAATATTTCTCCATTGATCGCGTCTTCCGAAATGAA
ACATTGGATGCCACACATTTGGCTGAGTTCCACCAAATAGAAGGGGTCATCGCCGACCACGGT
TTGACTCTTGGTCATTTGATGGGCGTATTGCGCGAATTTTTCACCAAACTGGGGATTACACAGC
TCCGATTTAAACCCGCATACAACCCTTACGGGGAGCCAAGTATGGAAGTGTTTAGCTATCACCA
GGGGCTCAAGAAGTGGGTTGAAGTGGGAAATTCAGGAGTCTTTAGGCCCGAGATGCTTCTTCC
AATGGGCCTGCCAGAAAACGTGTCAGTAATTGCATGGGGTCTCTCCCTCGAGAGACCCACAAT
GATAAAGTACGGAATTAATAACATACGCGAGTTGGTTGGGCACAAGGTAAACCTTCAGATGGTC

TATGACTCACCCGTCTGTAGACTTGATATAGAGCCTCGATCCAGCAAAACACAGGAGGCTGCCT
GATGATAA

MADNPVLELLLRRLEVADGGLDSAELATQLGVEHQAVVGAVKSLQALGEVIEAELRSTKCWELTTE
GEEIAREGSHEARVFRSIPLEGLVQSELMHLPSGKVGFSKAMSNKWIRVDKSAADGPRVFRVVDSIE
DEVQKRLQLVQAGQAEKLAEKERNELRKRKLLTEVILKTYWVSKGKAFSTSVSKQEAELSPEMISSG
SWRDRPFKPYNFSARGVLPDSGHLHPLLKVRSQFRQIFLEMGFTEMPTDNFIESSFWNFDALFQPQ
QHPARDQHDTFFLRDPAEALQLPMGYVQRVKRTHSQGGYGSQGYKYTWKLEEARKNLLRTHTTA
ASARALYQLAQKKPFTPAKYFSIDRVFRNETLDATHLAEFHQIEGVIADHGLTLGHLMGVLREFFTKL
GITQLRFKPAYNPYGEPSMEVFSYHQGLKKWVEVGNSGVFRPEMLLPMGLPENVSVIAWGLSLER
PTMIKYGINNIRELVGHKVNLQMVYDSPVCRLDIEPRSSKTQEAA***

***Hs*Phe$_{T413G}$**

ATGGCCGATGGGCAAGTGGCAGAGTTGCTCCTCCGGAGACTCGAGGCTAGTGACGGAGGACT
CGACAGCGCTGAGCTCGCTGCCGAACTGGGGATGGAGCACCAAGCCGTGGTCGGGGCTGTCA
AGAGCTTGCAGGCTTTGGGTGAAGTCATCGAGGCTGAACTCAGGAGCACCAAACACTGGGAAC
TCACAGCAGAAGGGGAAGAGATAGCTAGGGAAGGTAGCCACGAGGCTCGGGTTTTTCGCTCCA
TTCCACCCGAGGGACTTGCTCAGTCAGAACTCATGCGGCTTCCAAGTGGAAAAGTAGGATTTAG
CAAAGCTATGAGTAACAAGTGGATACGAGTCGATAAAAGCGCTGCCGACGGCCCACGCGTATT
CCGGGTGGTGGATAGCATGGAAGATGAAGTGCAGCGGAGGCTTCAGTTGGTTCGCGGAGGGC
AGGCAGAGAAACTTGGTGAGAAAGAGCGCTCAGAACTTCGGAAGAGGAAGCTGCTGGCCGAA
GTTACCCTGAAAACTTATTGGGTGAGTAAAGGCTCCGCCTTCAGTACCTCCATTTCCAAGCAGG
AAACCGAGTTGTCTCCAGAGATGATTAGTTCTGGAAGTTGGCGCGACAGGCCATTCAAGCCCTA
CAACTTTCTCGCACACGGTGTGCTTCCCGATTCAGGTCATCTGCACCCTCTCCTCAAAGTTAGA
TCACAGTTCCGCCAAATCTTTCTGGAGATGGGGTTCACCGAAATGCCTACAGATAACTTCATCG
AATCCAGCTTCTGGAATTTTGACGCACTGTTTCAGCCCCAACAACACCCCGCCAGAGATCAGCA
CGACACATTCTTCCTGCGAGACCCAGCCGAGGCTCTTCAGCTTCCAATGGATTATGTGCAGCG
CGTAAAAAGAACTCATAGTCAAGGCGGGTACGGAAGCCAGGGTTATAAGTACAATTGGAAACTG
GATGAAGCAAGGAAGAATCTCCTCCGCACACATACTACAAGTGCATCAGCCAGAGCCCTCTATC
GGCTCGCCCAAAAGAAGCCTTTTACCCCAGTGAAGTATTTTAGCATCGACCGGGTGTTCCGCAA
CGAGACACTGGATGCCACTCACCTGGCTGAATTTCACCAGATCGAAGGAGTGGTCGCCGACCA
CGGGTTGACACTGGGTCATTTGATGGGGGTGCTGCGAGAATTTTTTACTAAGCTGGGCATTACC
CAACTCCGATTCAAACCAGCTTATAACCCCTATGGAGAACCATCAATGGAAGTCTTCAGTTACCA
TCAAGGCCTCAAAAAGTGGGTTGAAGTCGGCAATTCCGGCGTCTTTCGACCTGAAATGCTGCTC
CCCATGGGGCTTCCTGAAAACGTTAGTGTAATAGCCTGGGGGTTGTCTCTTGAAAGGCCTACAA
TGATAAAATACGGGATTAATAATATCAGGGAGCTGGTTGGCCATAAAGTAAACTTGCAGATGGT
TTACGATAGCCCCCTTTGCAGGCTCGACGCCGAACCACGGCCCCCACCCACACAGGAAGCAG
CATGA

MADGQVAELLLRRLEASDGGLDSAELAAELGMEHQAVVGAVKSLQALGEVIEAELRSTKHWELTAE
GEEIAREGSHEARVFRSIPPEGLAQSELMRLPSGKVGFSKAMSNKWIRVDKSAADGPRVFRVVDSM
EDEVQRRLQLVRGGQAEKLGEKERSELRKRKLLAEVTLKTYWVSKGSAFSTSISKQETELSPEMISS
GSWRDRPFKPYNFLAHGVLPDSGHLHPLLKVRSQFRQIFLEMGFTEMPTDNFIESSFWNFDALFQP
QQHPARDQHDTFFLRDPAEALQLPMDYVQRVKRTHSQGGYGSQGYKYNWKLDEARKNLLRTHTT
SASARALYRLAQKKPFTPVKYFSIDRVFRNETLDATHLAEFHQIEGVVADHGLTLGHLMGVLREFFT
KLGITQLRFKPAYNPYTEPSMEVFSYHQGLKKWVEVGNSGVFRPEMLLPMGLPENVSVIAWGLSLE
RPTMIKYGINNIRELVGHKVNLQMVYDSPLCRLDAEPRPPPTQEAA***

Figure S2. Full-length gels for Figure 1(c) of the main text.

Full length fluorescent gels and protein loading controls for lysates from each mammalian cell type. After DIBO-Alexa Fluor 647 labeling and imaging for in-gel fluorescence, the relative amounts of protein loaded to each gel well were assessed via colloidal coomassie dye staining.

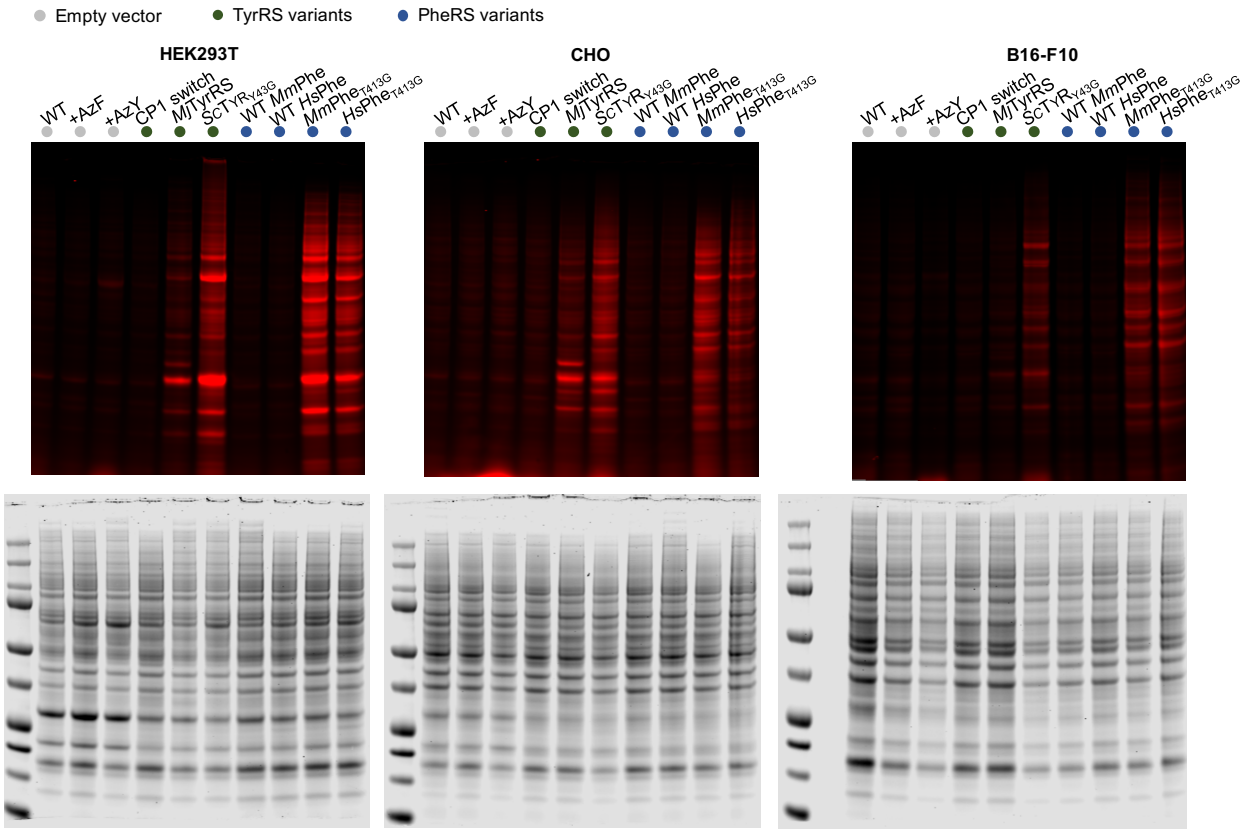

Figure S3. Full-length gels for Figure 1(d) and Figure 1(e) of the main text.

Full length fluorescent gels and protein loading controls for lysates exposed to increasing concentrations of endogenous or non-canonical amino acids for 24 hours. Endogenous amino acid titration was performed with 0.015 mM of either AzY or AzF. Quantification was performed using biological triplicates, adapting previously described methods.[2,3]

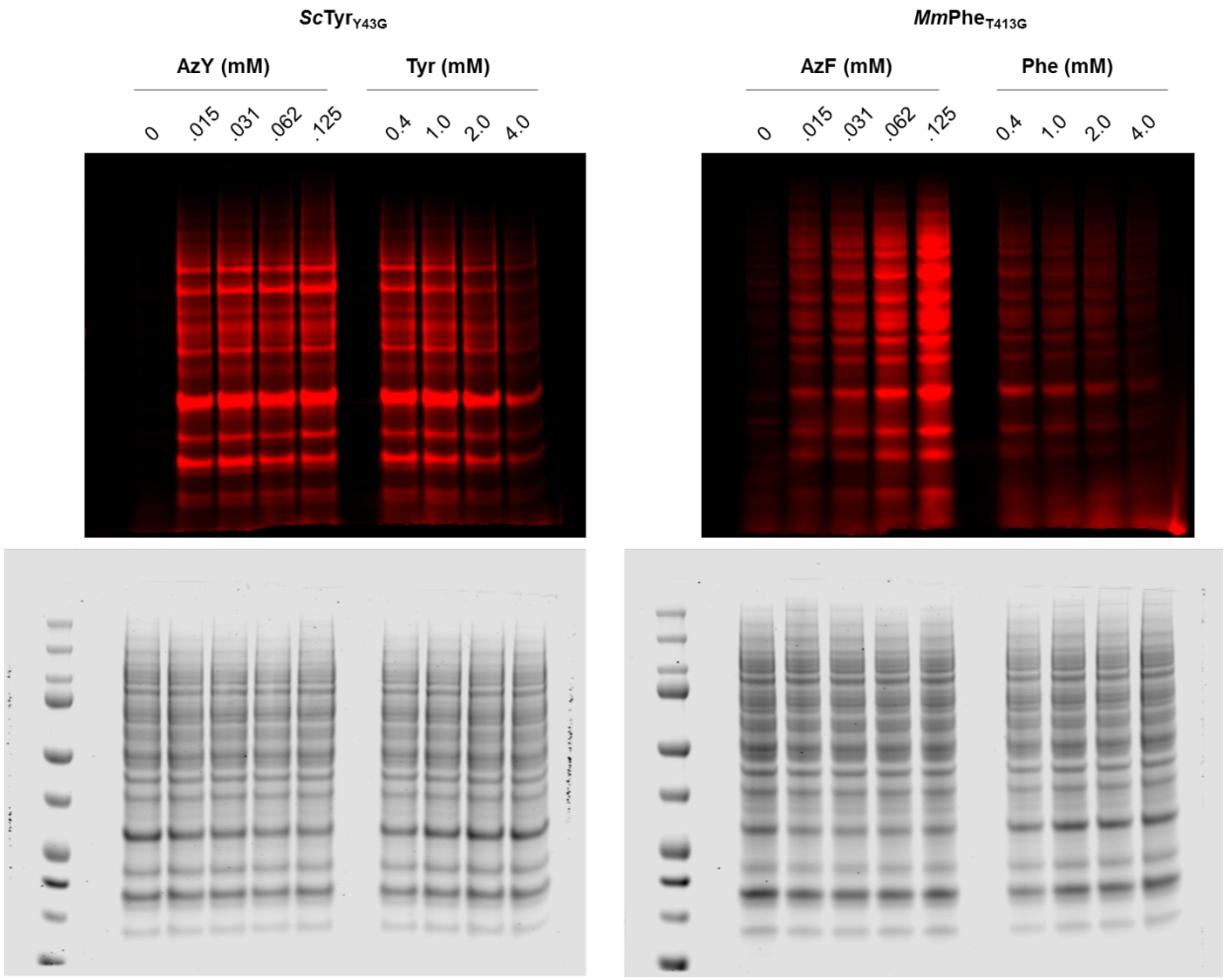

Figure S4. Single channel images from fluorescence confocal microscopy for Figure 2(a) of the main text.

Single channel fluorescence confocal images of *Sc*Tyr$_{Y43G}$ and *Mm*Phe$_{T413G}$-transfected HEK293T cells cultured with the non-canonical amino acids AzY and AzF, respectively. Images were obtained on a Zeiss LSM 880 microscope.

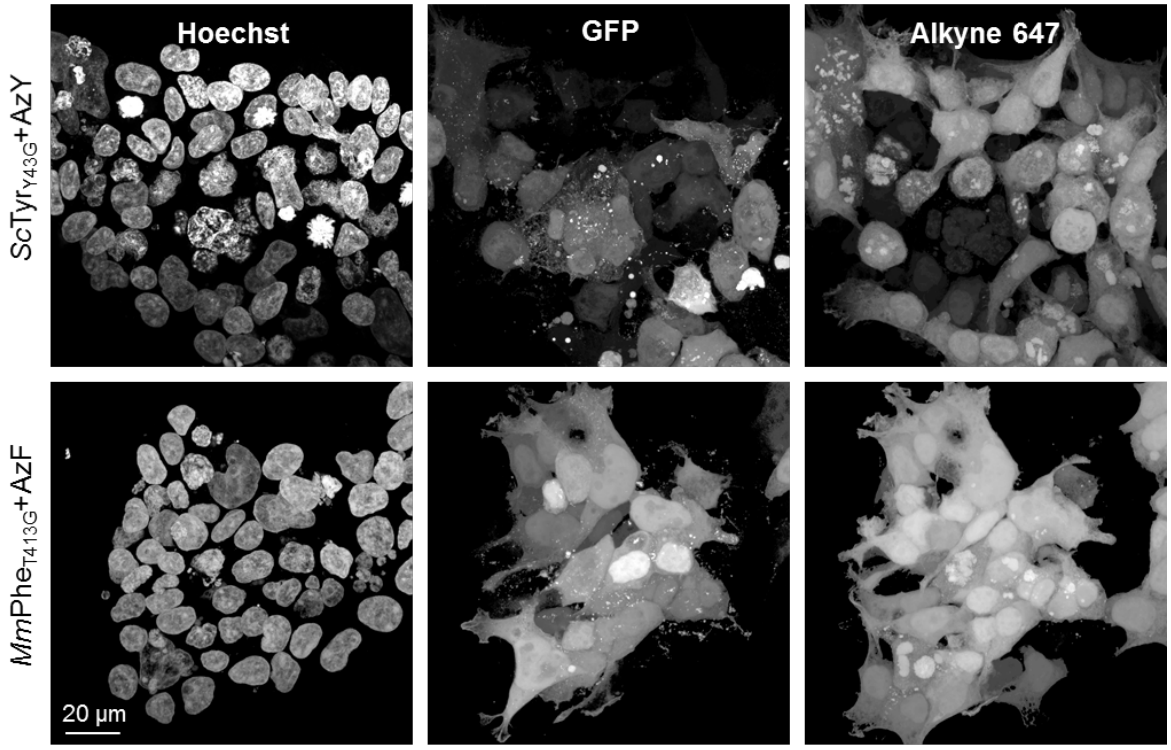

Figure S5. Gating strategy used in flow cytometry analysis in Figure 2(c) of the main text.

Gating strategy for fixed HEK293T cells pre-treated with iodoacetamide before reacting with DIBO Alexa Fluor 647. HEK293T cells were gated on a forward scatter (FSC) / side scatter (SSC) plot before live/ dead discrimination. Below is a representative gating, showing a biological replicate from *Sc*Tyr$_{Y43G}$-transfected, AzY-exposed cells. The FITC-647 plot shows data with the FlowJo default biexponential axis.

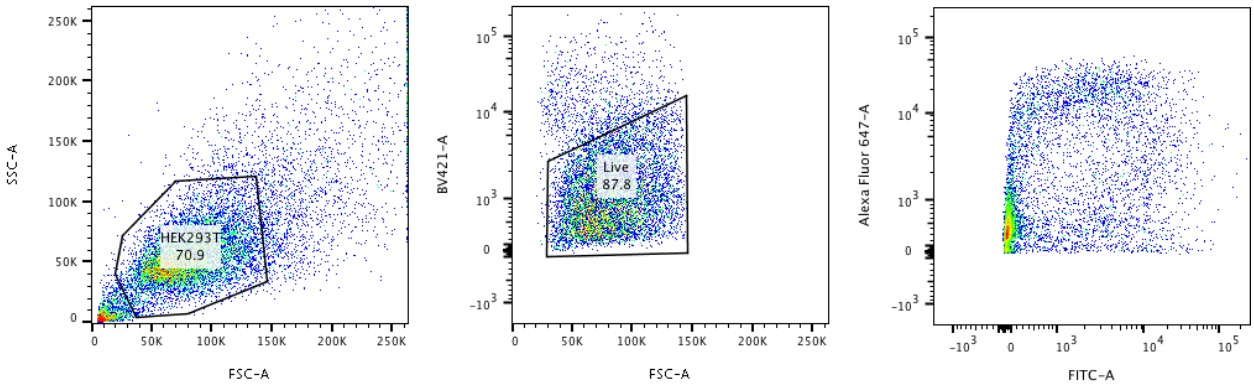

Figure S6. Volcano plots identifying proteome subsets quantified by each mutant aaRS over nonspecific background from negative controls.

In triplicate, HEK293T cells transfected with *Mm*Met$_{L274G}$, *Mm*Phe$_{T413G}$, and *Sc*Tyr$_{Y43G}$ were exposed to their corresponding ncAA: Anl, AzF, and AzF, respectively; or exposed to endogenous amino acids as negative controls to investigate background from nonspecific DBCO bead binding.

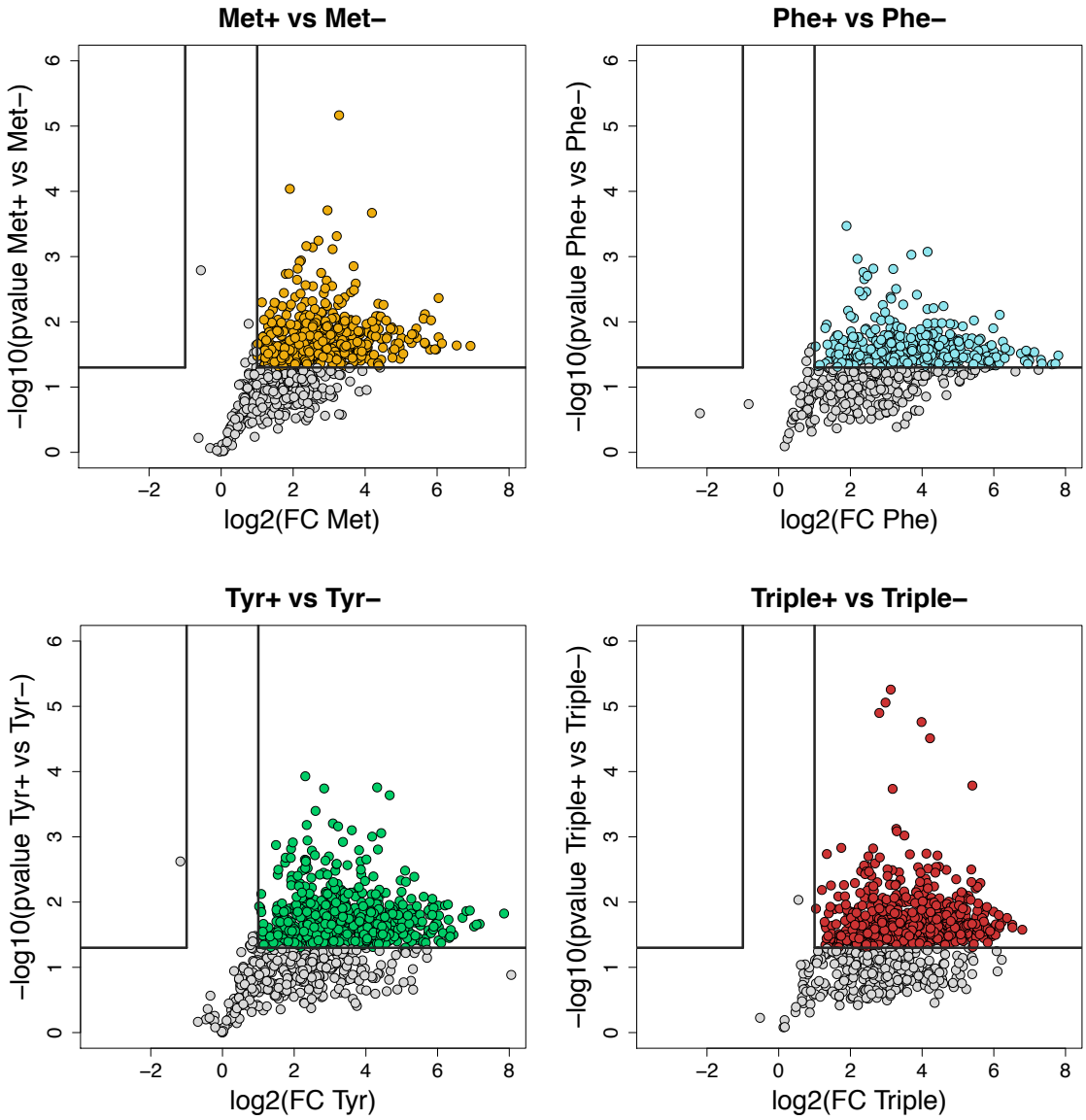

Figure S7. Pairwise comparison of proteome subsets preferentially labeled between single and triply expressed mutant aaRSs in HEK293T cells.

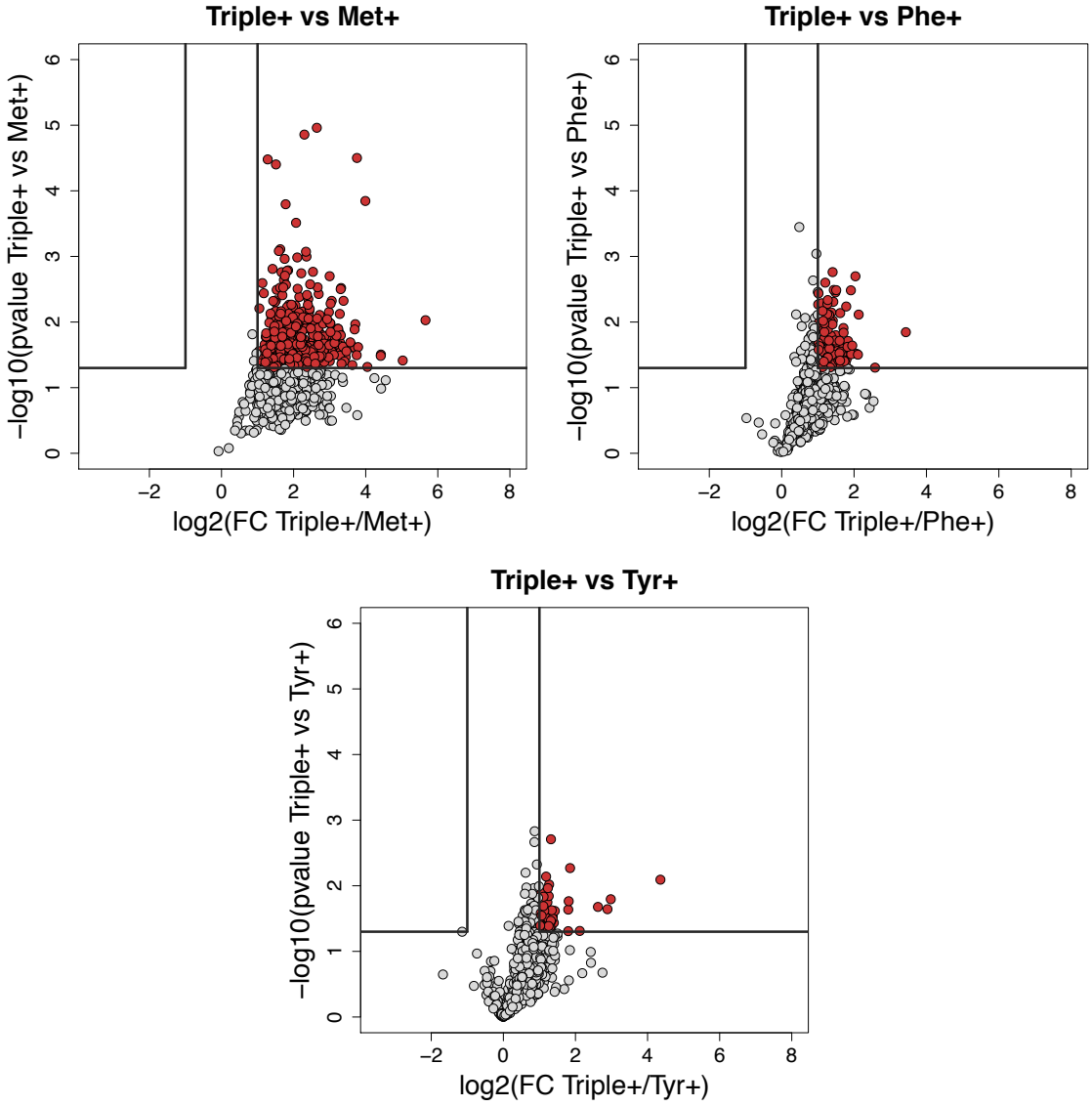

Figure S8. The frequency of Met, Phe, and Tyr codons only partially explains the enrichment efficiencies by *Mm*Met$_{L274G}$, *Mm*Phe$_{T413G}$, and *Sc*Tyr$_{Y43G}$, respectively.

The number of a cognate codon per protein, normalized by total protein length, weakly explains the mutant aaRS enrichment efficiency. The relative frequency of a target codon in a protein is plotted against the average enrichment fold-change between cells exposed to the ncAA (AnI, AzF, or AzY) or the canonical amino acid (Met, Phe, Tyr). Dotted lines indicate the 95% confidence interval of the least-square regression lines. These results are consistent with prior reports in *E. coli*,[13] suggesting that a combination of factors determine mutant aaRS enrichment efficiency.

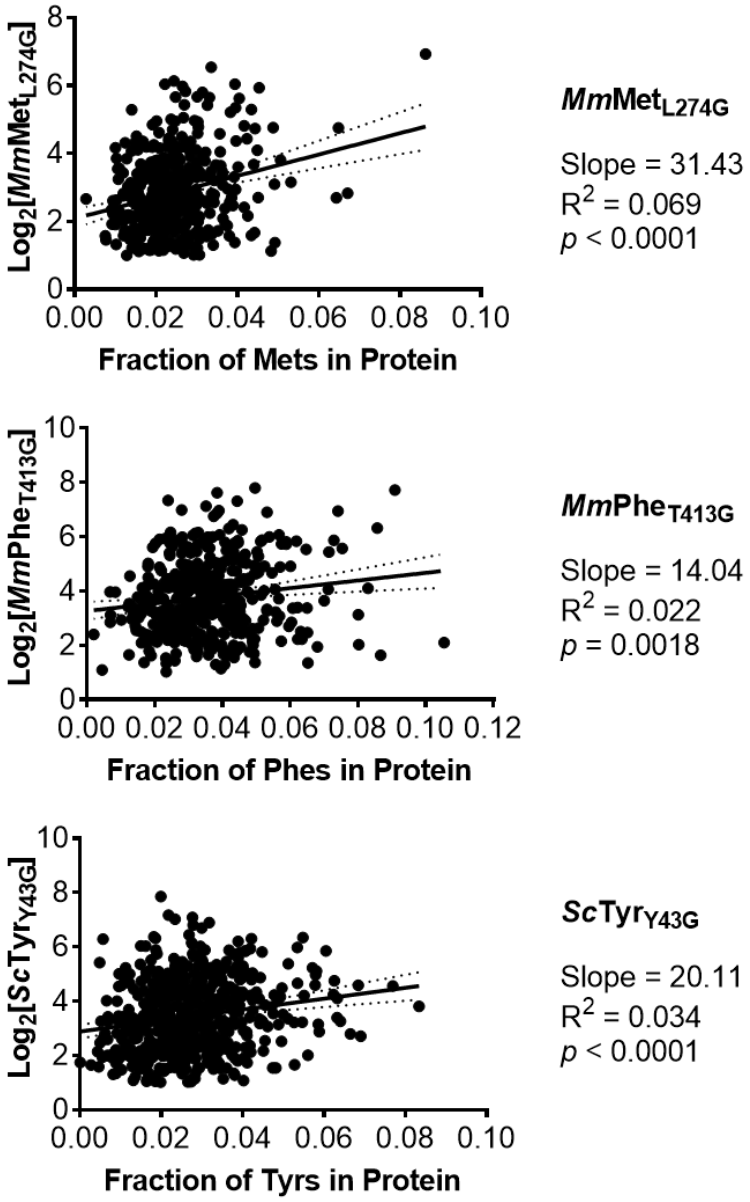

Figure S9. *Sc*Tyr$_{Y43G}$ and *Mm*Phe$_{T413G}$ label proteins via both of their cognate codons.

HEKT293T proteins containing exclusively one of the two cognate codons for tyrosine and phenylalanine were significantly enriched by *Sc*Tyr$_{Y43G}$ and *Mm*Phe$_{T413G}$, respectively, demonstrating that labeling can occur across codons. Proteins were TMT-labeled and quantified by mass spectrometry (Figure 3).

ScTyr$_{Y43G}$		MmPhe$_{T413G}$	
TAT	**TAC**	**TTT**	**TTC**
ALDOA	ACTG1	PHF6	H2AFX
CALM2	H2AFZ		HIST1H1D
CBX3	HSPA1B		HIST1H4J
CCT2	KNOP1		RPL13
GPATCH8	NME1-NME2		RPL28
HMGB1	RPL18		RPL32
LRRC59	RPL24		RPL36A
RPS14	RPL35		RPS6
RPS7	RPLP2		
RSL1D1	SERBP1		
ZC3H11A			

*Mm*Phe$_{T413G}$ preferentially labels the TTT codon, whereas *Sc*Tyr$_{Y43G}$ labels both its cognate codons equally. The tyrosine and phenylalanine codon fraction of *Sc*Tyr$_{Y43G}$- and *Mm*Phe$_{T413G}$-labeled proteins were compared with codon fractions of all TMT-identified proteins, including those not significantly enriched by *Sc*Tyr$_{Y43G}$+AzY and *Mm*Phe$_{T413G}$+AzF over +Y and +F negative controls. cDNA could be retrieved from Ensembl for 450 proteins enriched in *Sc*Tyr$_{Y43G}$+AzY, 352 proteins enriched in *Mm*Phe$_{T413G}$+AzF, and 1903 total proteins detected across TMT runs ('All') and used for this analysis. Data plotted as mean + SEM. *P < 0.05; t-test.

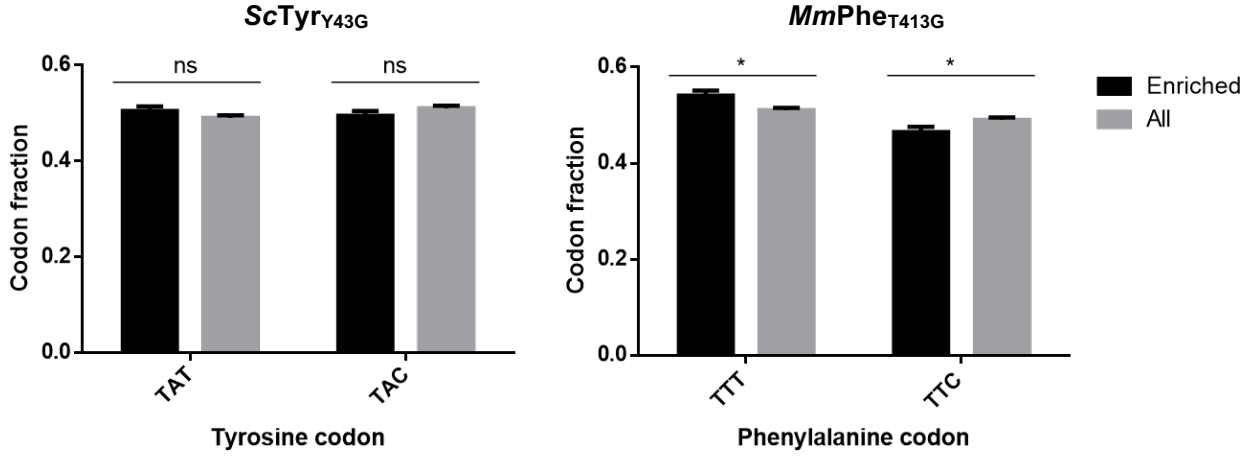

Figure S10. Single channel images from fluorescence confocal microscopy for Figure 4(a) of the main text.

Single channel fluorescence confocal images of B16-F10 melanoma xenografts stably expressing *Sc*Tyr$_{Y43G}$ and *Mm*Phe$_{T413G}$ exposed to the non-canonical amino acids AzY and AzF, respectively. Images were obtained on a Zeiss LSM 700 microscope.

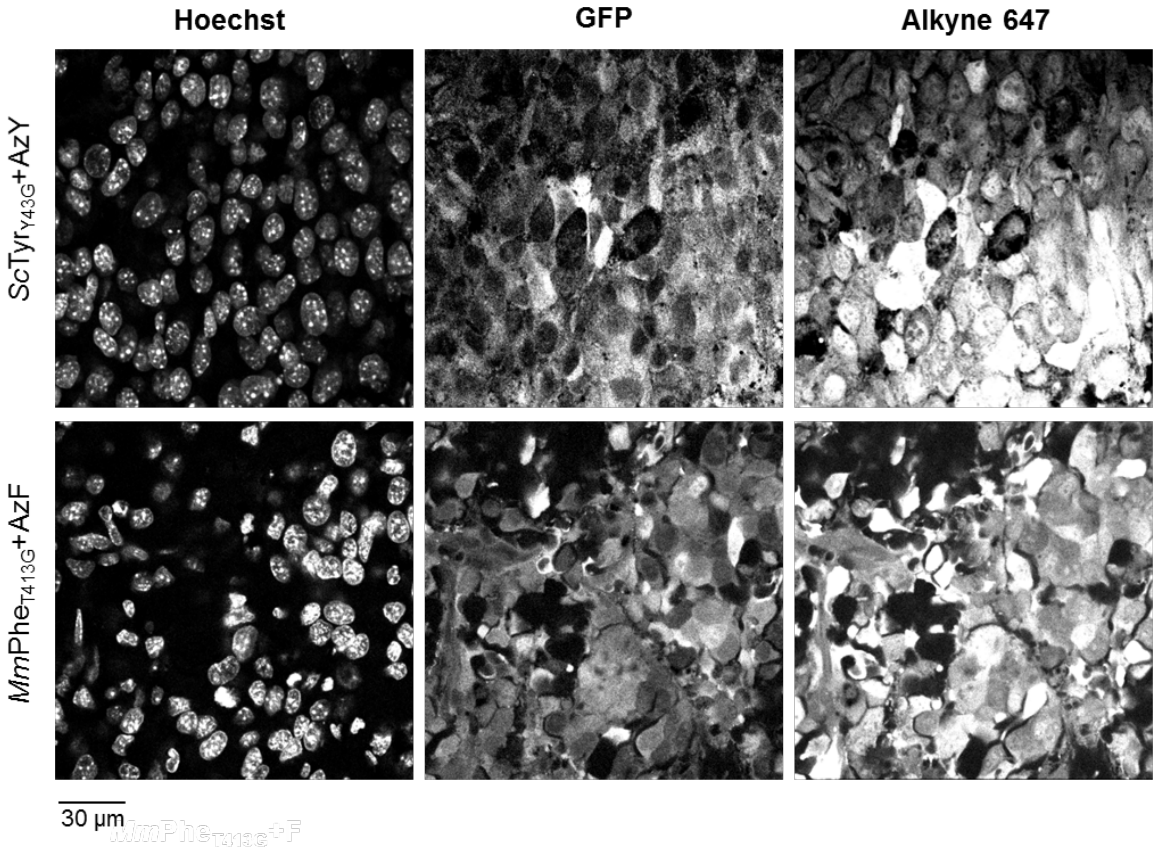

Figure S11. Full-length gel for Figure 4(b) of the main text.

Representative in-gel fluorescence of B16-F10 tumor lysates demonstrates proteome-wide incorporation of AzF and AzY by stably integrated *Mm*Phe$_{T413G}$ and *Sc*Ty$_{Y43G}$.

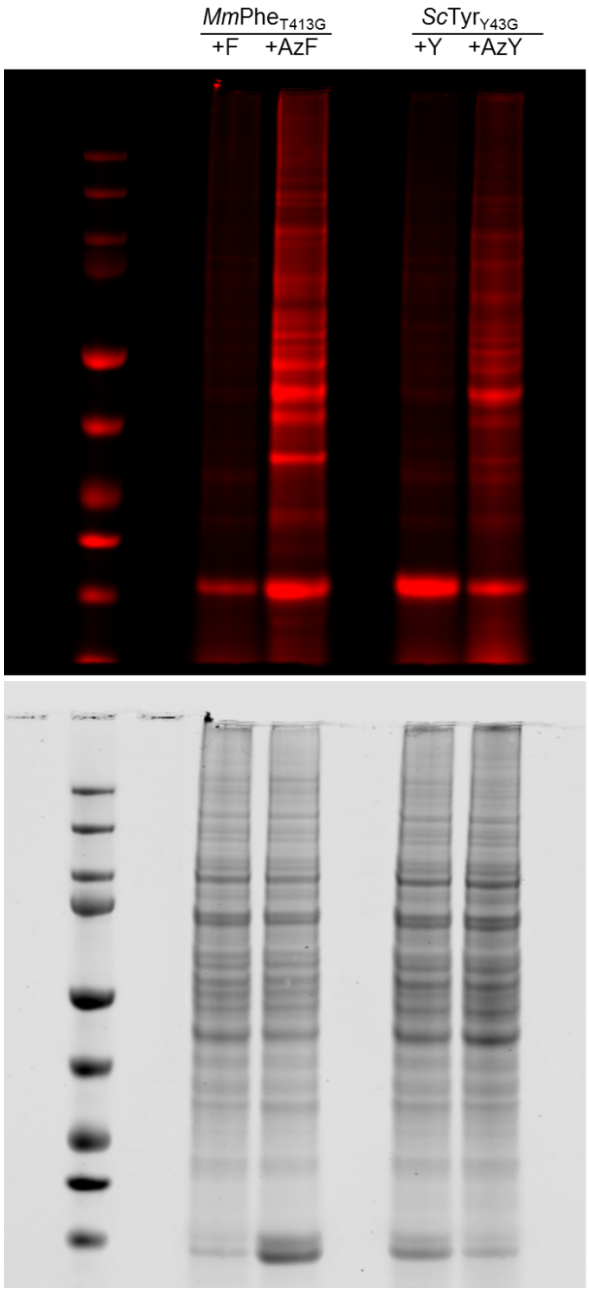

Figure S12. Enrichment of AzF- and AzY-incorporated B16-F10 melanoma proteomes and secretomes over nonspecific background (tumors exposed only to canonical Phe or Tyr amino acids). Melanoma cells stably expressed *Mm*Phe$_{T413G}$ or *Sc*Tyr$_{Y43G}$.

Melanoma lysate and secreted proteins are enriched via DBCO affinity purification in tumors exposed to azido-bearing AzF and AzY compared to those exposed to canonical Phe or Tyr.

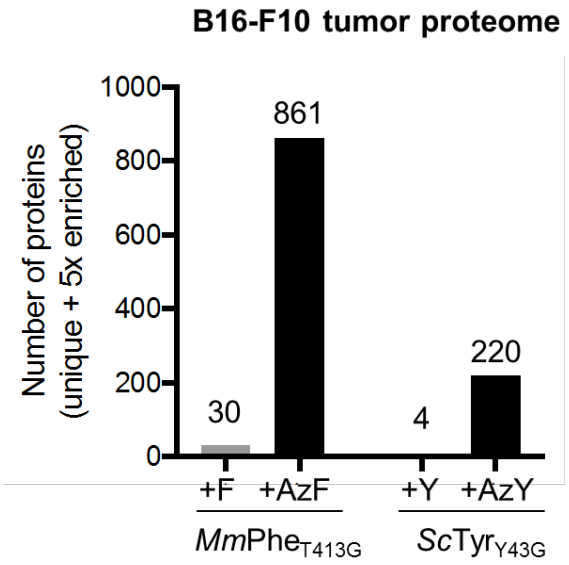

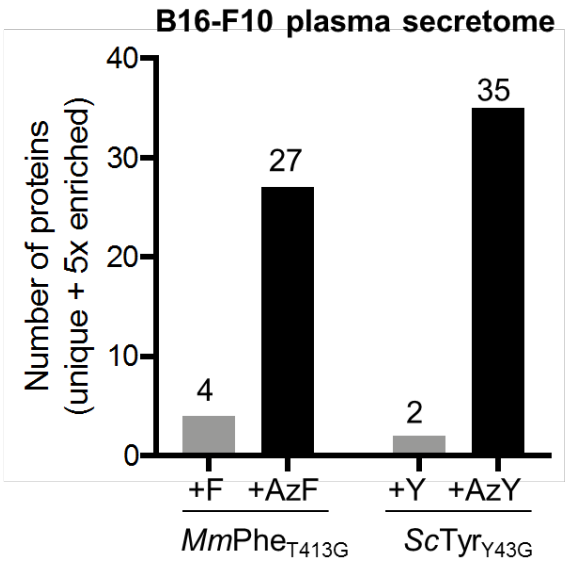

Figure S13. STRAP Gene ontology annotation by cellular components of *Mm*Phe$_{T413G}$ and *Sc*Tyr$_{Y43G}$ labeled *in vivo* melanoma proteomes in Figure 4(c) of the main text.

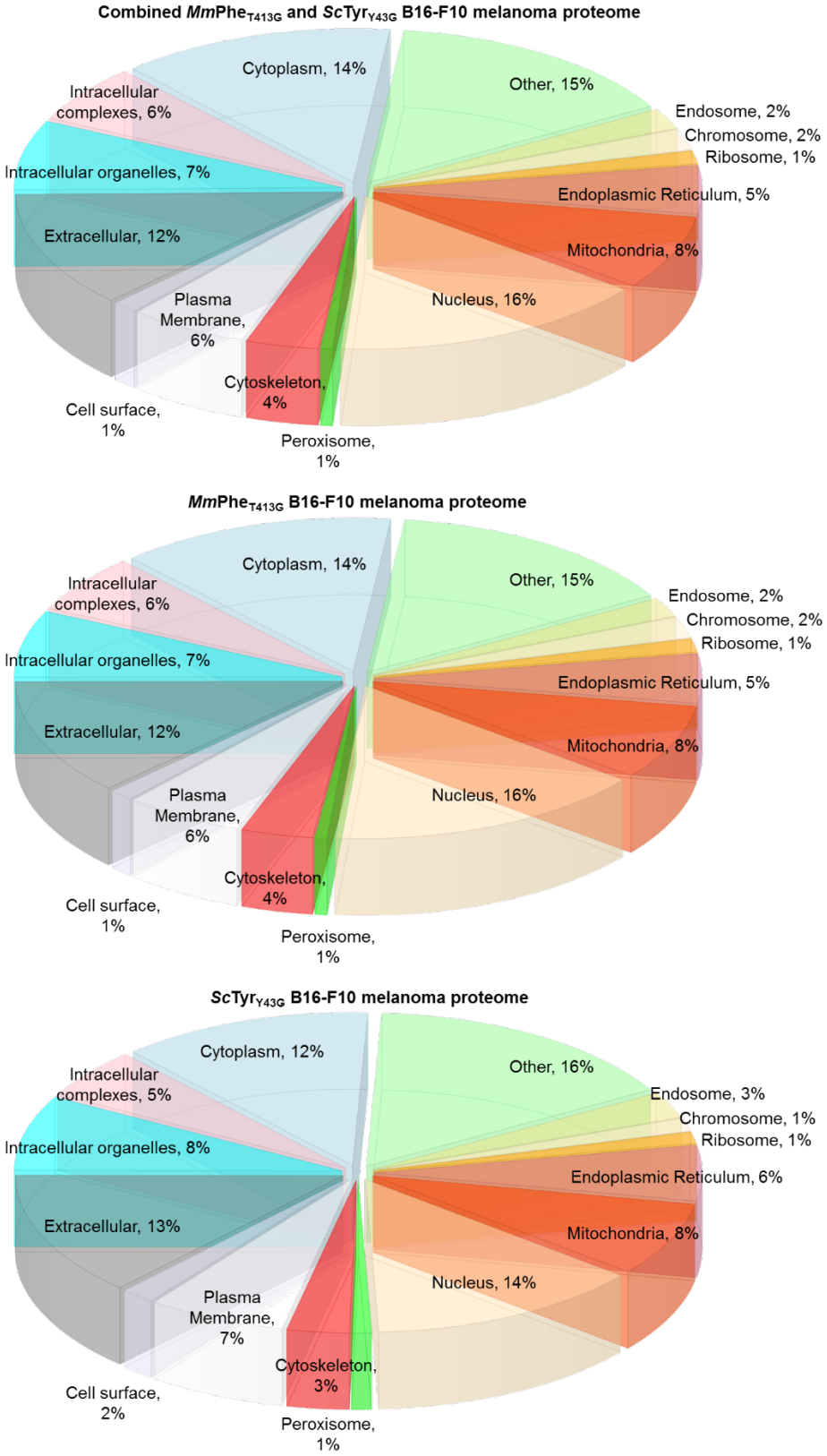

Figure S14. Ingenuity Pathway Analysis (Qiagen).

The top canonical pathways enriched in the labeled melanoma tumor proteome and secretome by *Mm*Phe$_{T413G}$ and *Sc*Tyr$_{Y43G}$. Figure 4(e) and 4(g) of the main text show enriched pathways with identifications from the two aaRSs combined.

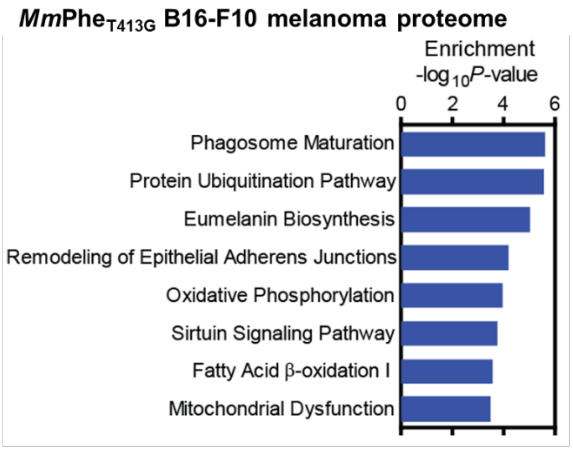

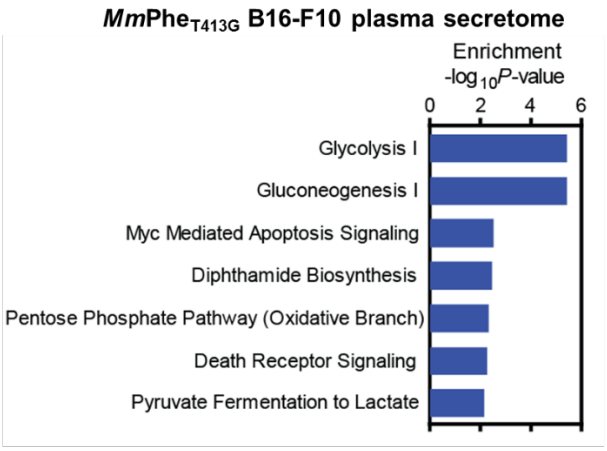

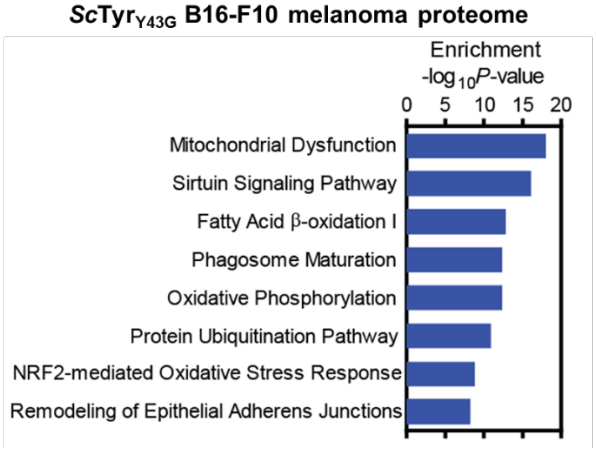

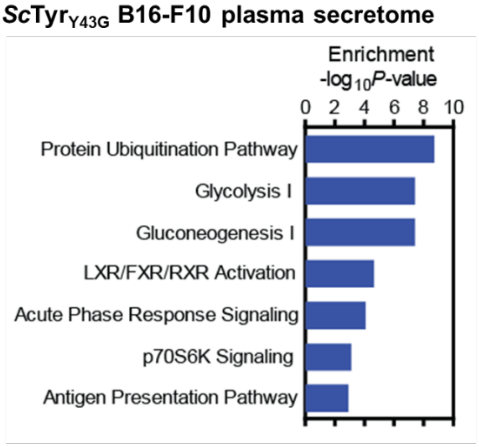

Figure S15. Low variability across B16-F10 *in vivo* labeled proteomes.

Reproducibility between biological replicates was assessed based on Proteome Discoverer's label-free quantification values across proteins detected in all replicates. Pearson correlation coefficients are displayed per replica pairwise comparison.

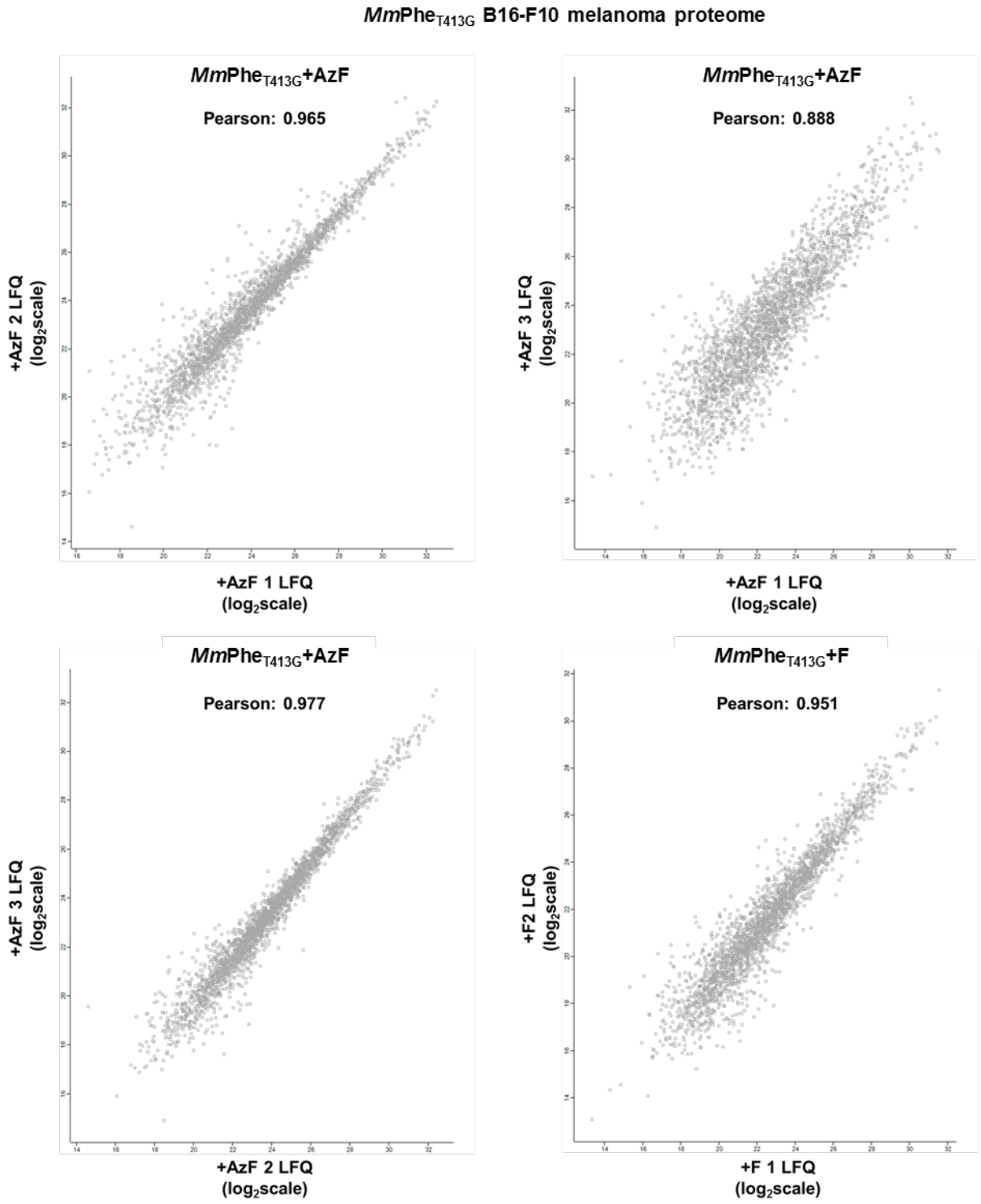

Figure S15 (continued). Low variability across B16-F10 *in vivo* labeled proteomes.

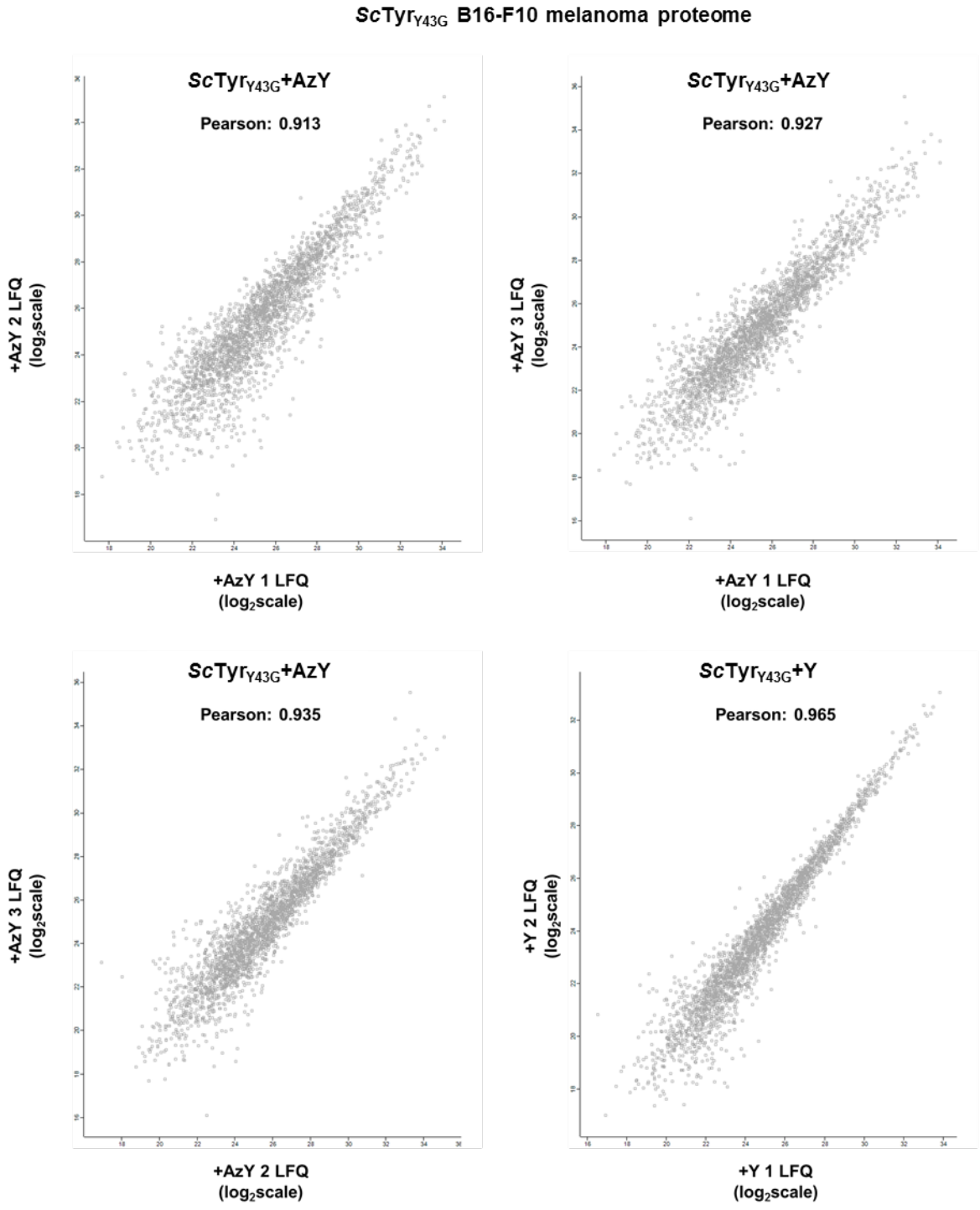

Figure S16. Low variability across B16-F10 *in vivo* labeled secretomes.

As in SF14, reproducibility between biological replicates was assessed based on Proteome Discoverer's label-free quantification values across proteins detected in all replicates. Pearson correlation coefficients are displayed per replica pairwise comparison.

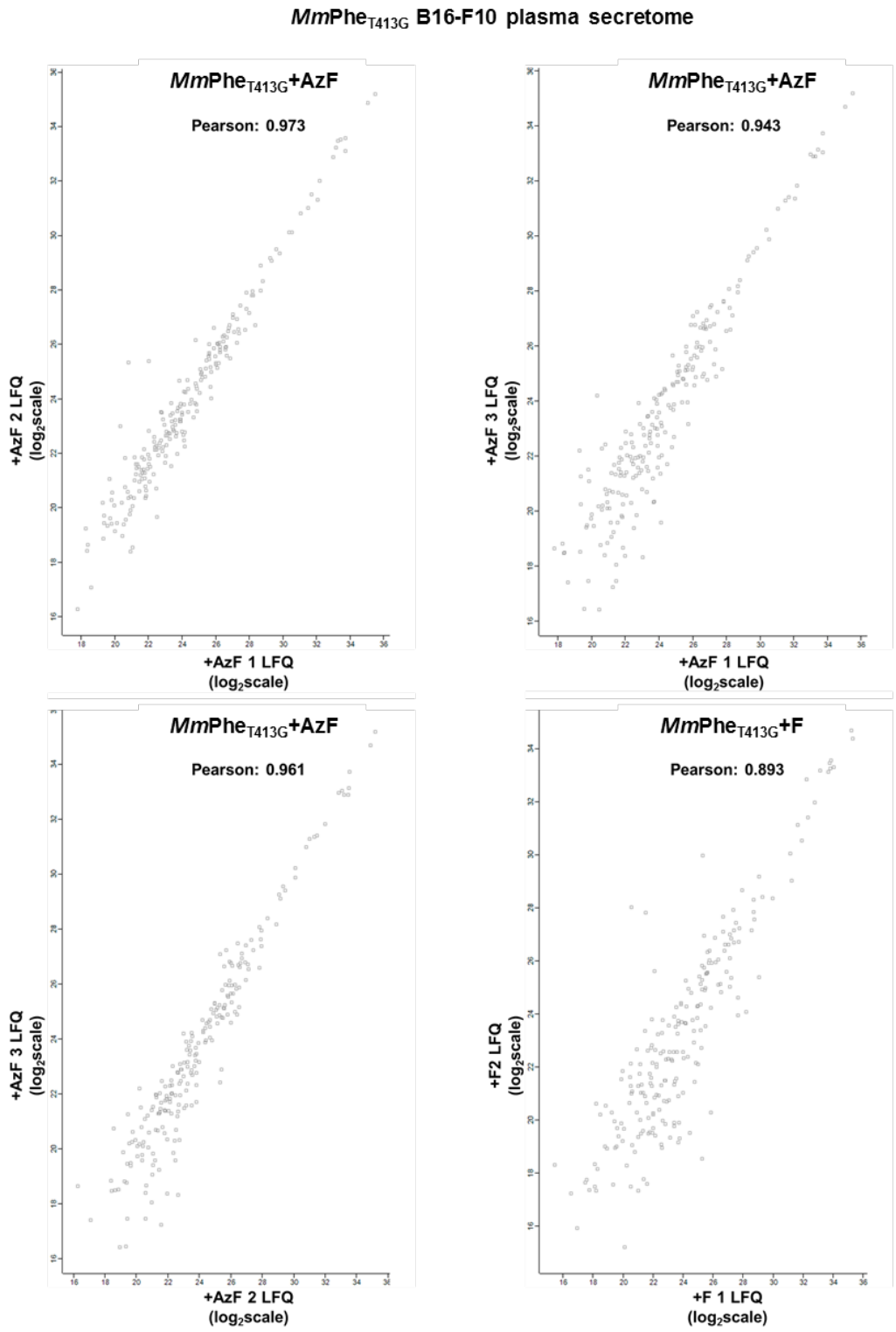

Figure S16 (continued). Low variability across B16-F10 *in vivo* labeled secretomes.

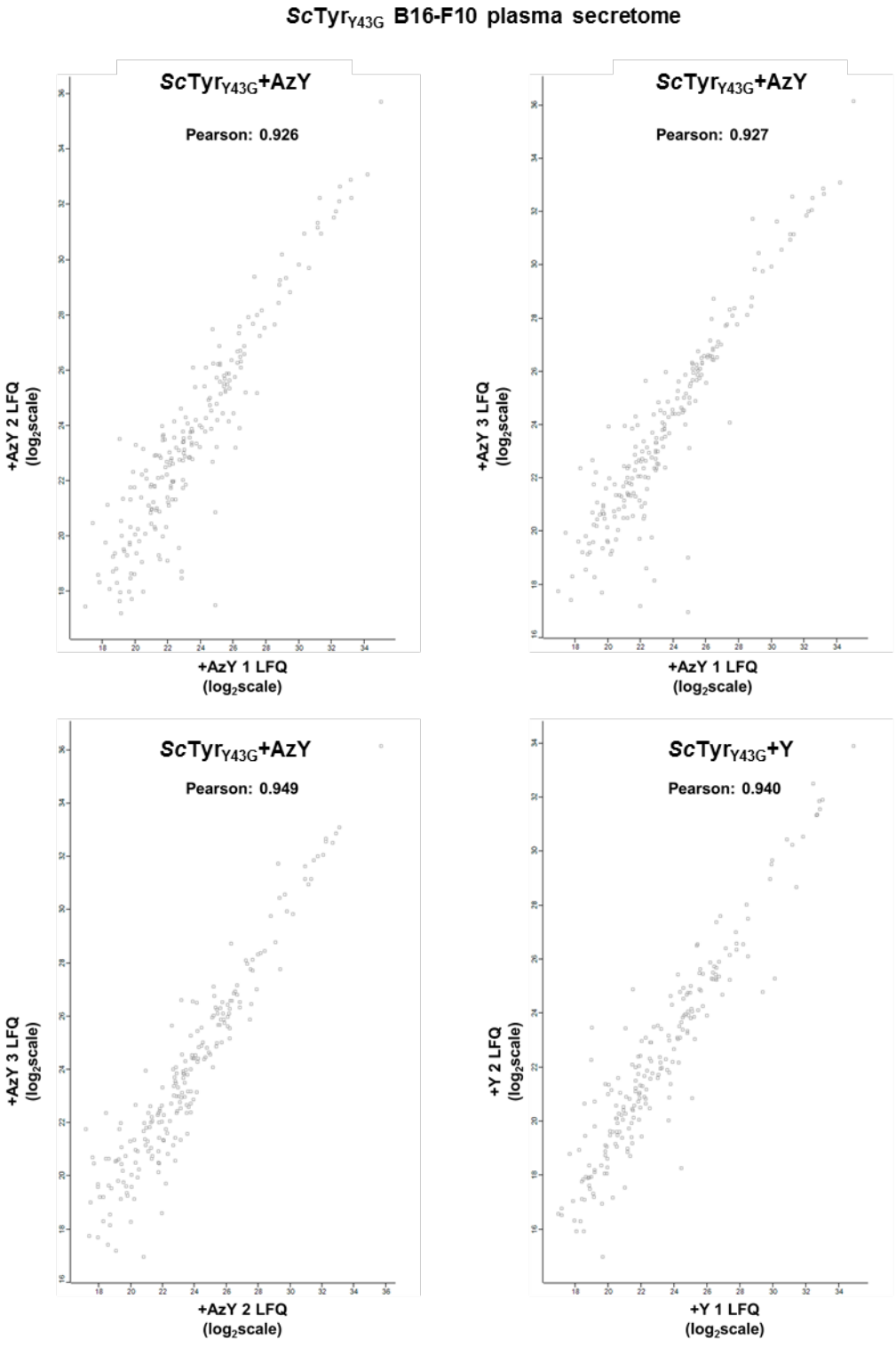

Supplementary Table 1. Labeled proteins secreted from B16-F10 melanomas into the plasma in Figure 4(f) of the main text.

Information on protein Function and Catalytic Activity are from the Gene Ontology database via the STRAP software. This table of proteins is also available in the Supporting Information proteomics Excel file.

Protein name	Gene	Uniprot ID	Identifying aaRS	Function	Catalytic Activity
14-3-3 protein gamma	*Ywhag*	P61982	*Sc*Tyr$_{Y43G}$	Adapter protein implicated in the regulation of a large spectrum of both general and specialized signaling pathways.	
14-3-3 protein theta	*Ywhaq*	P68254	*Mm*Phe$_{T413G}$	Adapter protein implicated in the regulation of a large spectrum of both general and specialized signaling pathways. Negatively regulates the kinase activity of PDPK1 (By similarity).	
5,6-dihydroxyindole-2-carboxylic acid oxidase	*Tyrp1*	P07147	*Mm*Phe$_{T413G}$	Catalyzes the oxidation of 5,6-dihydroxyindole-2-carboxylic acid (DHICA) into indole-5,6-quinone-2-carboxylic acid (PubMed:7813420).	
6-phosphogluconate dehydrogenase, decarboxylating	*Pgd*	Q9DCD0	*Mm*Phe$_{T413G}$	Catalyzes the oxidative decarboxylation of 6-phosphogluconate to ribulose 5-phosphate and CO(2), with concomitant reduction of NADP to NADPH.	6-phospho-D-gluconate + NADP(+) = D-ribulose 5-phosphate + CO(2) + NADPH.
78 kDa glucose-regulated protein	*Hspa5*	P20029	*Sc*Tyr$_{Y43G}$	Plays a role in facilitating the assembly of multimeric protein complexes inside the endoplasmic reticulum (PubMed:12475965).	
Actin, alpha cardiac muscle 1	*Actc1*	P68033	Both	Actins are highly conserved proteins that are involved in various types of cell motility and are	

				ubiquitously expressed in all eukaryotic cells.	
Alpha-1-antitrypsin 1-1	*Serpina1a*	P07758	*Sc*Tyr$_{Y43G}$	Inhibitor of serine proteases.	
Alpha-1-antitrypsin 1-2	*Serpina1b*	P22599	*Sc*Tyr$_{Y43G}$	Inhibitor of serine proteases.	
Alpha-1-antitrypsin 1-4	*Serpina1d*	Q00897	*Sc*Tyr$_{Y43G}$	Inhibitor of serine proteases.	
Alpha-1-antitrypsin 1-5	*Serpina1e*	Q00898	*Sc*Tyr$_{Y43G}$	Does not inhibit elastase or chymotrypsin.	
Alpha-enolase	*Eno1*	P17182	*Sc*Tyr$_{Y43G}$	Multifunctional enzyme that, as well as its role in glycolysis, plays a part in various processes such as growth control, hypoxia tolerance and allergic responses (By similarity).	2-phospho-D-glycerate = phosphoenolpyruvate + H(2)O.
Angiotensinogen	*Agt*	P11859	*Sc*Tyr$_{Y43G}$	Essential component of the renin-angiotensin system (RAS), a potent regulator of blood pressure, body fluid and electrolyte homeostasis.	
Antithrombin-III	*Serpinc1*	P32261	*Mm*Phe$_{T413G}$	Most important serine protease inhibitor in plasma that regulates the blood coagulation cascade.	
Aspartyl aminopeptidase	*Dnpep*	Q9Z2W0	*Sc*Tyr$_{Y43G}$	Aminopeptidase with specificity towards an acidic amino acid at the N-terminus.	Release of an N-terminal aspartate or glutamate from a peptide, with a preference for aspartate.
Carboxypeptidase N subunit 2	*Cpn2*	Q9DBB9	*Mm*Phe$_{T413G}$	The 83 kDa subunit binds and stabilizes the catalytic subunit at 37 degrees Celsius and keeps it in circulation.	

Complement C2	*C2*	P21180	*Mm*Phe$_{T413G}$	Component C2 which is part of the classical pathway of the complement system is cleaved by activated factor C1 into two fragments: C2b and C2a.	Selective cleavage of Arg-|-Ser bond in complement component C3 alpha-chain to form C3a and C3b, and Arg-|-Xaa bond in complement component C5 alpha-chain to form C5a and C5b.
Cytochrome c, somatic	*Cycs*	P62897	*Mm*Phe$_{T413G}$	Plays a role in apoptosis.	
Elongation factor 1-alpha 1	*Eef1a1*	P10126	*Sc*Tyr$_{Y43G}$	This protein promotes the GTP-dependent binding of aminoacyl-tRNA to the A-site of ribosomes during protein biosynthesis.	
Elongation factor 2	*Eef2*	P58252	Both	Catalyzes the GTP-dependent ribosomal translocation step during translation elongation.	
Fibulin-1	*Fbln1*	Q08879	*Mm*Phe$_{T413G}$	Incorporated into fibronectin-containing matrix fibers.	
Fibulin-5	*Fbln5*	Q9WVH9	*Mm*Phe$_{T413G}$	Essential for elastic fiber formation, is involved in the assembly of continuous elastin (ELN) polymer and promotes the interaction of microfibrils and ELN (By similarity).	
Glycerol-3-phosphate phosphatase	*Pgp*	Q8CHP8	*Sc*Tyr$_{Y43G}$	Glycerol-3-phosphate phosphatase hydrolyzing glycerol-3-phosphate into glycerol.	Glycerol 1-phosphate + H(2)O = glycerol + phosphate.
Histidine-rich glycoprotein	*Hrg*	Q9ESB3	*Sc*Tyr$_{Y43G}$	Plasma glycoprotein that binds a number of ligands such as heme, heparin, heparan sulfate, thrombospondin, plasminogen, and divalent metal ions.	

Histone H4	*Hist1h4a*	P62806	*Sc*Tyr$_{Y43G}$	Core component of nucleosome.	
Insulin-degrading enzyme	*Ide*	Q9JHR7	*Mm*Phe$_{T413G}$	Plays a role in the cellular breakdown of insulin, IAPP, glucagon, bradykinin, kallidin and other peptides, and thereby plays a role in intercellular peptide signaling.	Degradation of insulin, glucagon and other polypeptides. No action on proteins.
L-lactate dehydrogenase A chain	*Ldha*	P06151	Both		(S)-lactate + NAD(+) = pyruvate + NADH.
Leukotriene A-4 hydrolase	*Lta4h*	P24527	Both	Epoxide hydrolase that catalyzes the final step in the biosynthesis of the proinflammatory mediator leukotriene B4.	(7E,9E,11Z,14Z)-(5S,6S)-5,6-epoxyicosa-7,9,11,14-tetraenoate + H(2)O = (6Z,8E,10E,14Z)-(5S,12R)-5,12-dihydroxyicosa-6,8,10,14-tetraenoate.
Major urinary protein 2	*Mup2*	P11589	*Mm*Phe$_{T413G}$	Binds pheromones that are released from drying urine of males.	
Major urinary protein 3	*Mup3*	P04939	*Mm*Phe$_{T413G}$	Binds pheromones that are released from drying urine of males.	
Malate dehydrogenase, cytoplasmic	*Mdh1*	P14152	*Mm*Phe$_{T413G}$		(S)-malate + NAD(+) = oxaloacetate + NADH.
NADP-dependent malic enzyme	*Me1*	P06801	Both		Oxaloacetate = pyruvate + CO(2).
Nucleoside diphosphate kinase B	*Nme2*	Q01768	*Sc*Tyr$_{Y43G}$	Major role in the synthesis of nucleoside triphosphates other than ATP.	ATP + protein L-histidine = ADP + protein N-phospho-L-histidine.
Peptidyl-prolyl cis-trans isomerase A	*Ppia*	P17742	*Mm*Phe$_{T413G}$	PPIases accelerate the folding of proteins.	Peptidylproline (omega=180) = peptidylproline (omega=0).

Phosphoglycerate kinase 1	*Pgk1*	P09411	Both	In addition to its role as a glycolytic enzyme, it seems that PGK-1 acts as a polymerase alpha cofactor protein (primer recognition protein).	ATP + 3-phospho-D-glycerate = ADP + 3-phospho-D-glyceroyl phosphate.
Phosphoglycerate mutase 1	*Pgam1*	Q9DBJ1	*Sc*Tyr$_{Y43G}$	Interconversion of 3- and 2-phosphoglycerate with 2,3-bisphosphoglycerate as the primer of the reaction.	3-phospho-D-glyceroyl phosphate = 2,3-bisphospho-D-glycerate.
Phosphoribosylformylglycinamidine synthase	*Pfas*	Q5SUR0	*Sc*Tyr$_{Y43G}$	Phosphoribosylformylglycinamidine synthase involved in the purines biosynthetic pathway.	ATP + N(2)-formyl-N(1)-(5-phospho-D-ribosyl)glycinamide + L-glutamine + H(2)O = ADP + phosphate + 2-(formamido)-N(1)-(5-phospho-D-ribosyl)acetamidine + L-glutamate.
Proteasome subunit alpha type-1	*Psma1*	Q9R1P4	Both	Component of the 20S core proteasome complex involved in the proteolytic degradation of most intracellular proteins.	Cleavage of peptide bonds with very broad specificity.
Proteasome subunit alpha type-2	*Psma2*	P49722	Both	Component of the 20S core proteasome complex involved in the proteolytic degradation of most intracellular proteins.	Cleavage of peptide bonds with very broad specificity.
Proteasome subunit alpha type-4	*Psma4*	Q9R1P0	Both	Component of the 20S core proteasome complex involved in the proteolytic degradation of most intracellular proteins.	Cleavage of peptide bonds with very broad specificity.
Proteasome subunit beta type-1	*Psmb1*	O09061	*Sc*Tyr$_{Y43G}$	Component of the 20S core proteasome complex involved in the proteolytic degradation of most intracellular proteins.	Cleavage of peptide bonds with very broad specificity.

Proteasome subunit beta type-10	*Psmb10*	O35955	*Sc*Tyr$_{Y43G}$	The proteasome is a multicatalytic proteinase complex which is characterized by its ability to cleave peptides with Arg, Phe, Tyr, Leu, and Glu adjacent to the leaving group at neutral or slightly basic pH.	Cleavage of peptide bonds with very broad specificity.
Proteasome subunit beta type-5	*Psmb5*	O55234	*Sc*Tyr$_{Y43G}$	Component of the 20S core proteasome complex involved in the proteolytic degradation of most intracellular proteins.	Cleavage of peptide bonds with very broad specificity.
Proteasome subunit beta type-6	*Psmb6*	Q60692	*Sc*Tyr$_{Y43G}$	Component of the 20S core proteasome complex involved in the proteolytic degradation of most intracellular proteins.	Cleavage of peptide bonds with very broad specificity.
Protein/nucleic acid deglycase DJ-1	*Park7*	Q99LX0	*Sc*Tyr$_{Y43G}$	Protein and nucleotide deglycase that catalyzes the deglycation of the Maillard adducts formed between amino groups of proteins or nucleotides and reactive carbonyl groups of glyoxals.	An S-(1-hydroxy-2-oxopropyl)-[protein]-L-cysteine + H(2)O = a [protein]-L-cysteine + (R)-lactate.
Pyruvate kinase PKM	*Pkm*	P52480	*Mm*Phe$_{T413G}$	Glycolytic enzyme that catalyzes the transfer of a phosphoryl group from phosphoenolpyruvate (PEP) to ADP, generating ATP.	ATP + pyruvate = ADP + phosphoenolpyruvate.
Rab GDP dissociation inhibitor alpha	*Gdi1*	P50396	*Mm*Phe$_{T413G}$	Regulates the GDP/GTP exchange reaction of most Rab proteins by inhibiting the dissociation of GDP from them, and the subsequent binding of GTP to them.	
Serum amyloid A-1 protein	*Saa1*	P05366	*Sc*Tyr$_{Y43G}$	Major acute phase reactant.	

Serum amyloid A-2 protein	*Saa2*	P05367	*Sc*Tyr$_{Y43G}$	Major acute phase reactant.	
Serum paraoxonase/arylesterase 1	*Pon1*	P52430	*Mm*Phe$_{T413G}$	Hydrolyzes the toxic metabolites of a variety of organophosphorus insecticides.	An N-acyl-L-homoserine lactone + H(2)O = an N-acyl-L-homoserine.
Transketolase	*Tkt*	P40142	*Sc*Tyr$_{Y43G}$	Catalyzes the transfer of a two-carbon ketol group from a ketose donor to an aldose acceptor, via a covalent intermediate with the cofactor thiamine pyrophosphate.	Sedoheptulose 7-phosphate + D-glyceraldehyde 3-phosphate = D-ribose 5-phosphate + D-xylulose 5-phosphate.
Transthyretin	*Ttr*	P07309	*Sc*Tyr$_{Y43G}$	Thyroid hormone-binding protein.	
Triosephosphate isomerase	*Tpi1*	P17751	Both		D-glyceraldehyde 3-phosphate = glycerone phosphate.
UTP--glucose-1-phosphate uridylyltransferase	*Ugp2*	Q91ZJ5	*Mm*Phe$_{T413G}$	Plays a central role as a glucosyl donor in cellular metabolic pathways.	UTP + alpha-D-glucose 1-phosphate = diphosphate + UDP-glucose.

Supplementary References

[1] Wakasugi, K.; Quinn, C.L.; Tao, N.; Schimmel P. Genetic code in evolution: switching species-specific aminoacylation with a peptide transplant. *The EMBO Journal*. 1998 Jan 1;17(1):297-305.
[2] Thesis: Mahdavi, Alborz. Ph.D. Dissertation, California Institute of Technology, Pasadena, CA, 2015.
[3] Mahdavi, A.; Hamblin, GD.; Jindal, GA.; Bagert, JD.; Dong, C.; Sweredoski, MJ.; Hess, S.; Schuman, EM.; Tirrell, DA. Engineered aminoacyl-tRNA synthetase for cell-selective analysis of mammalian protein synthesis. *Journal of the American Chemical Society*. 2016 Mar 25;138(13):4278-81.
[4] Lund, R.; Leth-Larsen, R.; Jensen, ON.; Ditzel, HJ. Efficient isolation and quantitative proteomic analysis of cancer cell plasma membrane proteins for identification of metastasis-associated cell surface markers. *Journal of proteome research*. 2009 Apr 27;8(6):3078-90.
[5] Zhang, L.; Elias, JE. Relative protein quantification using tandem mass tag mass spectrometry. *Proteomics: Methods and Protocols*. 2017:185-98.
[6] Eng, JK.; McCormack, AL.; Yates, JR. An approach to correlate tandem mass spectral data of peptides with amino acid sequences in a protein database. *Journal of the American Society for Mass Spectrometry*. 1994 Nov 1;5(11):976-89.
[7] Käll, L.; Canterbury, JD.; Weston, J.; Noble, WS.; MacCoss, MJ. Semi-supervised learning for peptide identification from shotgun proteomics datasets. *Nature methods*. 2007 Nov;4(11):923.
[8] Dray, S.; Dufour, AB. The ade4 package: implementing the duality diagram for ecologists. *Journal of statistical software*. 2007 Jan;22(4):1-20.
[9] Tyanova, S.; Temu, T.; Sinitcyn, P.; Carlson, A.; Hein, MY.; Geiger, T.; Mann, M.; Cox, J. The Perseus computational platform for comprehensive analysis of (prote) omics data. *Nature methods*. 2016 Sep;13(9):731.
[10] Alvarez-Castelao, B.; Schanzenbächer, CT.; Hanus, C.; Glock, C.; tom Dieck, S.; Dörrbaum, AR.; Bartnik, I.; Nassim-Assir, B.; Ciirdaeva, E.; Mueller, A.; Dieterich DC. Cell-type-specific metabolic labeling of nascent proteomes in vivo. *Nature biotechnology*. 2017 Dec;35(12):1196.
[11] Bhatia, VN.; Perlman, DH.; Costello, CE.; McComb, ME. Software tool for researching annotations of proteins: open-source protein annotation software with data visualization. *Analytical chemistry*. 2009 Oct 19;81(23):9819-23.
[12] Krämer, A.; Green, J.; Pollard, Jr J.; Tugendreich, S. Causal analysis approaches in ingenuity pathway analysis. *Bioinformatics*. 2013 Dec 13;30(4):523-30.
[13] Elliott, TS.; Bianco, A.; Townsley, FM.; Fried, SD.; Chin, JW. Tagging and enriching proteins enables cell-specific proteomics. *Cell chemical biology*. 2016 Jul 21;23(7):805-15.